HHS Public Access

Author manuscript

Nature. Author manuscript; available in PMC 2020 August 12.

Published in final edited form as:

Nature. 2020 February ; 578(7795): 461–466. doi:10.1038/s41586-020-2000-y.

NEDD8 nucleates a multivalent cullin-RING-UBE2D ubiquitin ligation assembly

Kheewoong Baek[1], **David T. Krist**[1,2], **J. Rajan Prabu**[1], **Spencer Hill**[3], **Maren Klügel**[1], **Lisa-Marie Neumaier**[1], **Susanne von Gronau**[1], **Gary Kleiger**[3], **Brenda A. Schulman**[1,*]

[1]Department of Molecular Machines and Signaling, Max Planck Institute of Biochemistry, Martinsried, 82152, Germany

[2]Present address: Carl R. Woese Institute for Genomic Biology, University of Illinois at Urbana-Champaign, Urbana, IL, USA

[3]Department of Chemistry and Biochemistry, University of Nevada, Las Vegas, Las Vegas, NV, 89154, USA

Abstract

Virtually all eukaryotic processes are regulated by cullin-RING E3 ligase (CRL)-catalyzed protein ubiquitylation[1], which is exquisitely controlled by cullin modification with the ubiquitin (UB)-like protein NEDD8[2–6]. However, how CRLs catalyze ubiquitylation, and the basis for NEDD8 activation, remain unknown. We report the cryo EM structure of a chemically-trapped complex representing the ubiquitylation intermediate whereby neddylated CRL1$^{\beta\text{-TRCP}}$ promotes UB transfer from the E2 UBE2D to its recruited substrate phosphorylated IκBα. The structure shows that NEDD8 acts as a nexus binding disparate cullin elements and the RING-activated UB-linked UBE2D. Concomitant local structural remodeling and large-scale CRL domain movements converge to juxtapose the substrate and ubiquitylation active site. The results explain how a distinctive UB-like protein alters the functions of its targets, and show how numerous NEDD8-dependent interprotein interactions and conformational changes synergistically configure a catalytic CRL architecture that is both robust for rapid substrate ubiquitylation and fragile to enable ensuing cullin-RING functions.

Cullin-RING E3 ubiquitin (UB) ligases (CRLs) orchestrate an astounding array of eukaryotic processes, including transcription, signaling, cell division, and differentiation, whereas CRL dysregulation underlies many pathologies. This immense impact depends on coordinated but dynamic interactions between dedicated cullin-RING complexes and several

*Corresponding author: schulman@biochem.mpg.de.

Author contributions

KB, DTK, MK, LN, and SvG generated protein complexes and assayed quality for suitability for cryo EM. DTK conceived of, designed, and generated stable proxies for ubiquitylation intermediates. KB, DTK, SH, and GK performed ubiquitylation assays. KB and JRP collected, processed, and refined cryo EM data and built and refined structure. KB, DTK, GK and BAS prepared manuscript with input from other authors. BAS supervised the project.

Competing Interests Declaration

The authors declare no competing interests.

regulatory partner proteins[1]. Cullins (CULs) 1–5 bind cognate RING-containing partners (RBX1 or RBX2) through a conserved intermolecular Cullin/RBX (hereafter "C/R") domain, where a CUL β-sheet stably embeds an RBX strand[7]. On one side of the C/R domain, the CUL N-terminal domain can associate interchangeably with numerous substrate-recruiting receptors. As examples, human CUL1-RBX1 binds ≈70 SKP1-F-box protein complexes, while CUL4-RBX1 binds ≈30 DDB1-DCAF complexes, forming "CRL1$^{\text{F-box protein name}}$" or "CRL4$^{\text{DCAF name}}$" E3s, respectively[8–11]. The C-terminal CUL "WHB" and RBX "RING" domains emanate from the other side of the C/R domain. To achieve E3 ligase activity, the RING recruits one of multiple UB-carrying enzymes, which presumably use distinct mechanisms to transfer UB to receptor-bound substrates.

CRLs are regulated by reversible NEDD8 modification of a specific Lys within the CUL WHB domain. Despite ≈60% identity to UB, NEDD8 uniquely activates CRL-dependent ubiquitylation[2]. NEDD8 has been suggested to play multiple roles in catalysis, including assisting in the recruitment of ubiquitin carrying enzymes, facilitating juxtaposition of the substrate and ubiquitylation active site, and promoting conformational changes, although the structural mechanisms for these effects remain elusive[3–5,12]. NEDD8 also stabilizes cellular CRLs by blocking the exchange factor CAND1 from ejecting substrate receptors from unneddylated CUL-RBX complexes[13]. Neddylation controls ≈20% of UB-mediated proteolysis and presumably many non-degradative functions of UB, and an inhibitor (MLN4924/Pevonedistat™) is in anti-cancer clinical trials and blocks HIV infectivity[6,14].

Here we determine structural mechanisms underlying ubiquitylation by human neddylated CRL1$^{\beta\text{-TRCP}}$ and a UBE2D-family E2, with the F-box protein β-TRCP recruiting a specific phosphodegron motif in substrates including β-catenin and IκBα[15–20]. UBE2D knockdown stabilizes the CRL1$^{\beta\text{-TRCP}}$ substrate IκBα[21], while mutations impairing CRL1$^{\beta\text{-TRCP}}$ ubiquitylation of β-catenin promote tumorigenesis[22]. Furthermore, hijacking of CRL1$^{\beta\text{-TRCP}}$ enables HIV to evade host immunity[23], and NEDD8 Gln40 deamidation by an enteropathogenic and enterohemorrhagic *Escherichia coli* effector results in accumulation of the CRL1$^{\beta\text{-TRCP}}$ substrate IκBα as well as substrates of other CRLs[24–26].

NEDD8 activation of ubiquitylation

Kinetic parameters for CRL1$^{\beta\text{-TRCP}}$ and UBE2D-catalyzed ubiquitylation of model substrates (phosphopeptides from β-catenin and IκBα, harboring single acceptor lysines), determined by rapid quench-flow methods, showed NEDD8 massively stimulates the reaction, by nearly 2000-fold overall (Figure 1a, Extended Data Figure 1, Extended Data Table 1). Performing experiments under conditions allowing multiple UBE2D turnover events enabled probing for effects on substrate "priming", whereby UB is ligated directly to substrate, versus chain elongation. Quantifying individual rates for linkage of successive UBs during polyubiquitylation showed NEDD8 activates both reactions. However, 10-fold slower UB linkage to a substrate-linked UB suggests neddylated CRL1$^{\beta\text{-TRCP}}$ together with UBE2D optimally catalyzes substrate priming (Extended Data Table 1).

Cryo EM reveals Cullin-RING dynamics

UB transfer from a RING-docked UBE2D~UB intermediate ("~" indicates thioester bond/thioester-bond mimic) to an F-box protein-bound substrate is difficult to rationalize by prior structural models[3,7,20,27], or by our cryo EM reconstructions of unneddylated and neddylated substrate-bound CRL1$^{\beta\text{-TRCP}}$ (Extended Data Figure 2, Extended Data Table 2). A well-resolved "substrate scaffolding module" resembles models based on crystal structures of substrate-bound SKP1-β-TRCP and the portion of an F-box-SKP1-CUL1-RBX1 complex including CUL1's N-terminal domain and the intermolecular C/R domain[7,20]. However, for RBX1's RING and CUL1's WHB domains, with or without covalently-linked NEDD8, density is lacking or visualized only at low contour, in varying positions in different classes. These domains apparently sample multiple orientations, and it is thus difficult to conceptualize rapid ubiquitylation of a flexible substrate by uncoordinated nanometer-scale motions of RBX1-activated UBE2D~UB (Extended Data Figure 2).

Capturing CRL substrate ubiquitylation

Substrate priming involves fleeting simultaneous linkage of UBE2D's active site, UB's C-terminus, and the substrate (Figure 1b). We chemically adjoined surrogates for these entities in a stable mimic of the transition state, which avidly binds neddylated CRL1$^{\beta\text{-TRCP}}$ (Figure 1c, Extended Data Figure 3a–d). After screening several complexes by cryo EM, we obtained a reconstruction at 3.7 Å resolution showing our proxy for a UBE2D~UB-IκBα substrate intermediate bound to a hyperactive version of neddylated CRL1$^{\beta\text{-TRCP}}$ (Figure 2a, Extended data Figures 3, 4, Extended Data Table 2).

Our complex representing the neddylated CRL1$^{\beta\text{-TRCP}}$-UBE2D~UB-substrate intermediate explains rapid ubiquitylation through unprecedented neddylated cullin-RING arrangements (Extended Data Figure 5). NEDD8 is nearly encircled by interactions, binding its linked CUL1 WHB domain in an "activation module", and positioning a "catalytic module" relative to the substrate scaffolding module to juxtapose the active site and substrate (Figure 2b–d).

In the catalytic module, RBX1 binds UBE2D~UB in the canonical RING-activated "closed" conformation, where noncovalent UBE2D and UB interactions allosterically activate the thioester bond between them[28–30]. Compared to prior isolated RING-UBE2D~UB structures[28–30], the neddylated CRL1$^{\beta\text{-TRCP}}$-UBE2D~UB-substrate intermediate shows additional density corresponding to the substrate proxy along a trajectory to the ubiquitylation active site (Figure 2c, Extended data Figure 6a). A UBE2D groove appears to engage the substrate polypeptide poised to assist in projecting adjacent lysines into the active site. This may contribute to UBE2D's ability to ubiquitylate a broad range of substrates[31].

The structurally-observed ≈22 angstroms between IκBα's β-TRCP-bound phosphodegron and the UBE2D~UB active site is compatible with spacing between this motif and potential acceptor lysines in many substrates[32] (Extended Data Figure 6) and predicts: 1) peptide substrates with sufficient residues (e.g. 13 and 9) between the phosphodegron and acceptor

Lys to span ≈22 Å should be rapidly primed in a NEDD8-dependent manner; 2) a peptide substrate with too few spacer residues (e.g. 4) to span this gap should be severely impaired for priming by neddylated CRL1$^{\beta\text{-TRCP}}$ and UBE2D, but addition of a UB could satisfy geometric constraints and enable further polyubiquitylation; and 3) the substrates should show little difference in UBE2D-mediated priming with unneddylated CRL1$^{\beta\text{-TRCP}}$. Comparing kinetic parameters for peptide substrates with 13-, 9-, and 4-residue spacers confirms these predictions, with the latter peptide reducing the priming rate with neddylated CRL1$^{\beta\text{-TRCP}}$ to below that we could quantify (Extended Data Figure 6, Extended Data Table 1).

NEDD8 orchestrates UB ligation assembly

NEDD8 and its covalently-linked CUL1 WHB domain form a globular activation module. A NEDD8 groove, comprising the Ile36/Leu71/Leu73 hydrophobic patch and the C-terminal tail, embraces the hydrophobic face of the isopeptide-bound CUL1 helix (Figure 2d, 3a–b). At the center, NEDD8's Gln40 contacts CUL1, the isopeptide bond, and NEDD8's C-terminal tail in a buried polar interaction typical of those organizing apolar interfaces[33]. This rationalizes how pathogenic bacterial effectors catalyzing Gln40 deamidation impair CRL1-dependent ubiquitylation[12,24–26]: the resultant negative charge would shatter the CUL1-NEDD8 interface.

The activation module binds the catalytic module, solving the mystery of how neddylation helps CRL1$^{\beta\text{-TRCP}}$ recruit UBE2D in cells[34]. NEDD8's Ile44 hydrophobic patch engages UBE2D's "backside", opposite from the ubiquitylation active site (Figure 3c, Extended Data Figure 7a). Contacts resemble those described for free NEDD8 or UB binding to UBE2D's backside, and allosterically stimulating intrinsic reactivity of an isolated RING-UBE2D~UB subcomplex[35–38]. We examined intrinsic reactivity by monitoring UB discharge to free lysine using a previously-described hyperactive neddylated CRL1$^{\beta\text{-TRCP}}$ mutant[39] and high enzyme and lysine concentrations. Substrate-independent UB transferase activity was impaired by a NEDD8 mutant disrupting the integrity of the activation module, and by UBE2D mutations hindering interactions with its covalently-linked UB, RBX1's RING domain or NEDD8 (Extended Data Figure 7c–f). Thus, the architecture observed in the neddylated CRL1$^{\beta\text{-TRCP}}$-UBE2D~UB-substrate complex structure may both stimulate intrinsic reactivity of the UBE2D~UB intermediate and place the catalytic center in proximity of the β-TRCP-bound substrate.

The activation module is itself positioned by NEDD8 binding the substrate scaffolding module. NEDD8's Leu2, Lys4, Glu14, Asp16, Arg25, Arg29, Glu32, Gly63 and Gly64, which nestle in a concave CUL1 surface, vary in UB and account for nearly one-third of sequence differences between them (Figure 3d). Their UB counterparts would be predicted to repel CUL1, rationalizing a need for NEDD8 as a distinctive UB-like protein.

In addition, the catalytic module abuts both CUL1-RBX1 and substrate-receptor sides of the substrate scaffolding module (Figure 3e, Extended Data Figure 5). On one side, RBX1's RING stacks on its C/R domain Trp35 side-chain, consistent with previously reported effects

for RBX1 Trp35Ala mutation[39]. On the other side, UBE2D's curved β-sheet complements β-TRCP's propeller (Figure 3e).

NEDD8 conformation coincidence coupling

Although different conformations of UB and UB-like proteins have long been recognized to influence contacts, with UB-binding domains selecting between "Loop-in" or "Loop-out" orientations of the Leu8-containing β1/β2-loop, how these conformations might simultaneously impact multiple interactions is largely unknown[40]. Our data show NEDD8 must adopt the Loop-out conformation to both form the activation module and to engage UBE2D in the catalytic module (Figure 3f, Extended Data Figure 7g–i). NEDD8's conformation apparently serves as a coincidence detector, coupling noncovalent binding to its linked CUL1 WHB domain and to the catalytic module.

Synergistic catalytic assembly

The importance of structurally-observed interfaces was tested by effects of mutations in an attenuated pulse-chase assay format that qualitatively, but exclusively, monitors NEDD8-activated substrate priming by CRL1$^{β\text{-}TRCP}$ and UBE2D (Extended Data Figure 8). Mutations designed to destroy the activation module (NEDD8 Q40E) or hinder interactions between the activation and catalytic modules (NEDD8 I44A or UBE2D S22R) substantially impair substrate priming, as does swapping key NEDD8 residues at the interface with the substrate scaffolding module with those in UB. Moreover, although the structural basis for ubiquitylation by other CRLs awaits future studies, the mutations also impair UBE2D-mediated priming of a Cyclin E phosphopeptide substrate with neddylated CRL1^{FBW7}, and of IKZF zinc finger 2 by neddylated CRL4$^{CRBN/Pomalidomide}$ (Extended Data Figure 8g–n).

Given that the neddylated CRL1$^{β\text{-}TRCP}$-UBE2D~UB-substrate intermediate depends on multiple conformational changes and large interfaces within and between modules (Figure 2, Extended Data Figures 5, 7), we hypothesized that pairing mutations impacting various interfaces would have synergistic effects. Defining kinetic parameters for peptide substrate ubiquitylation with two types of experiments (K_m measured by titrating UBE2D, and rate constant k_{obs} for UB transfer determined by rapid quench-flow at saturating UBE2D concentrations to isolate catalytic defects) suggested three major conclusions (Figure 4a, Extended Data Figure 1, Extended Data Table 1). First, although no individual mutation is as detrimental as eliminating neddylation, mutation of each interface has a roughly 10-fold or greater effect on its own. The worst "single" mutation is NEDD8 substitution with UB (R72A), confirming the importance of NEDD8 and interactions between the activation and substrate scaffolding modules. The second worst is Q40E, underscoring the significance of the structure of the activation module and its role in establishing NEDD8's Loop-out conformation. Second, combining mutations at multiple sites is devastating, even for mild mutations. For example, the NEDD8 I44A mutation that is ≈10-fold defective on its own, combined with the UBE2D H32A mutation at the catalytic module-substrate receptor interface that is mildly defective in an attenuated assay with sub-saturating UBE2D (Extended Data Figure 8f), is nearly 200-fold defective. Third, the mutations have comparatively little effect on chain extension, consistent with the neddylated CRL1$^{β\text{-}TRCP}$-

UBE2D~UB-substrate intermediate structure defining UB transfer from UBE2D directly to unmodified substrate.

Discussion

Our cryo EM structure representing the neddylated CRL1$^{\beta\text{-TRCP}}$-UBE2D~UB-substrate intermediate suggests a model for substrate priming that solves many longstanding mysteries. First, rapid substrate ubiquitylation can be explained by NEDD8, the cullin and RBX1-bound UBE2D~UB making numerous interactions that activate UBE2D and synergistically place the catalytic center adjacent to β-TRCP. Second, perplexing neddylated CRL features incompatible with prior structures are now rationalized, including NEDD8-stimulated crosslinking between a CRL1$^{\beta\text{-TRCP}}$-bound phosphopeptide and UBE2D[4]; simultaneous NEDD8 linkage to a cullin and binding to the backside of RBX1-bound UBE2D[3,7,37]; and catastrophic effects of bacterial effector-catalyzed NEDD8 Gln40 deamidation[24–26] (Figure 2, 3). Third, residues in UB differing from NEDD8 would clash in the catalytic architecture (Figure 3d, Extended Data Table 1), thus rationalizing the existence of NEDD8 as a distinct UB-like protein.

In the absence of other factors, neddylated CRL1$^{\beta\text{-TRCP}}$'s scaffolding module robustly bridges the substrate with the C/R domain, while NEDD8, it's linked CUL1 WHB and RBX1's RING domain are relatively dynamic, apparently waving around (Extended data Figure 2). These mobile entities are harnessed in the neddylated CRL1$^{\beta\text{-TRCP}}$-UBE2D~UB-substrate intermediate (Figure 2). The numerous requisite protein-protein interactions and conformational changes suggest there could be multiple routes to the catalytic architecture (Figure 4b), where formation of interfaces successively narrows the range of options, akin to progression down a free energy funnel. Because ubiquitylation does occur with mutant substrates or enzymes, albeit at substantially lower rates (Extended Data Table 1), we cannot exclude that UB could be transferred from RING- and NEDD8-bound UBE2D in various orientations relative to the substrate-scaffolding module. However, if the thioester bond is both in the RING-activated configuration and adjacent to substrate as in the structure, this would increase the rate at which the presumably random exploration of three-dimensional space by a substrate lysine would lead to productive collision with the active site. Accordingly, blunting any single contribution to the structurally-observed catalytic architecture increases the relative importance of other contacts – even lesser ones (Figure 4a, Extended Data Table 1).

While neddylated CRL1$^{\beta\text{-TRCP}}$ and UBE2D seem optimal for UB priming of peptide-like substrates, the limited effect of the mutations on linkage of subsequent UBs (Extended Data Table 1) raises the possibility that different forms of ubiquitylation involve alternative, presently elusive, catalytic architectures. Although not overtly observed for our substrates with a single acceptor Lys, one question is if there are other circumstances when a substrate-linked UB could mimic NEDD8 and activate further ubiquitylation. Moreover, in addition to UBE2D, neddylated CRLs recruit a range of other UB-carrying enzymes, from ARIH-family RBR E3s for substrate priming to other E2s for polyubiquitylation[21,41–43], and UBXD7, which in turn recruits the AAA-ATPase p97 to process some ubiquitylated substrates[44]. We speculate that these CRL partners uniquely harness the dynamic NEDD8,

its linked CUL WHB and/or the RBX1 RING to specify distinct catalytic activities, much like the thioester-linked UBE2D~UB intermediate captures neddylated CRL1$^{\beta\text{-TRCP}}$ through multiple surfaces to specify substrate priming. The malleability of neddylated CRLs, coupled with numerous UB carrying enzyme partners, may underlie successful molecular glue or PROTAC-targeted protein degradation, while potential limits in their multivalent catalytic architectures may explain failures in such chemically-directed ubiquitylation of heterologous substrates[45]. Additionally, it seems likely that the conformational dynamics of unneddylated CRLs (Extended Data Figure 2) would enable transitioning between the different conformations coordinating cycles of neddylation/deneddylation with CAND1-driven substrate-receptor exchange[39,46–49]. Thus, the multifarious nature of interactions and conformations determining robust and rapid substrate priming, revealed by the structure of the neddylated CRL1$^{\beta\text{-TRCP}}$-UBE2D~UB-substrate intermediate, also provides a mechanism by which common elements can be transformed by different protein partners to interconvert between distinct CRL assemblies meeting the cellular demand for ubiquitylation.

Methods

Cloning, Protein Expression, & Purification

All proteins are of human origin. All variants of UBE2D2, UBE2D3, UBE2M, RBX1, CUL1, CUL4, NEDD8, and UB were generated using PCR, Quikchange (Agilent), or synthesized by Twist Biosciences.

UBE2D2 was purified as previous described[50], and UBE2D3 was purified in a similar manner. UB was expressed in BL21(DE3) RIL as previous described[51]. Wild type CUL1, RBX1(5-C), SKP1, β-TRCP2, CUL4A (from residue 38 to C-terminus, hereafter referred to as CUL4), CRBN, DDB1, and UBA1 were cloned into pLIB vectors[52]. GST-TEV-RBX1 and CUL1, GST-TEV-RBX1 and CUL4A, His-TEV-β-TRCP2 and SKP1 or His-TEV-DDB1 and CRBN were co-expressed by co-infecting with two baculoviruses. UBA1 was cloned with an N-terminal GST-tag with a TEV cleavage site. These proteins were expressed in *Trichoplusia ni* High-Five insect cells, purified by either GST or nickel affinity chromatography, overnight TEV cleavage, followed by ion exchange and size exclusion chromatography. All variants of CUL1-RBX1 were purified similarly. Purification of NEDD8, UBE2M, APPBP1-UBA3, SKP1-FBW7 (from residue 263 to C-terminus[53]), neddylation of CUL1-RBX1, and fluorescent labeling of Ubiquitin (UB) used for biochemical assays were performed as previously described[39]. β-TRCP1 (monomeric form, from residue 175 to C-terminus[20], hereafter referred to as β-TRCP1) with an N-terminal His-MBP followed by a TEV cleavage site was cloned into a pRSFDuet vector with "SKP1$^{\Delta\Delta}$" (SKP1 harboring two internal deletions, of residues 38–43 and 71–82)[54]. SKP1ΔΔ-β-TRCP1 was expressed in BL21(DE3) Gold *E. coli* at 18°C, purified with nickel affinity chromatography, followed by TEV cleavage, anion exchange, and size exclusion chromatography. Modification of RBX1-CUL1 and RBX1-CUL4A by UB instead of NEDD8 was performed with the UB R72A mutant that allows its activation and conjugation by neddylating enzymes APPBP1-UBA3 and UBE2M[55,56]. The reaction for ubiquitylating CUL4A-RBX1 was performed at pH 8.8 to drive the reaction to completion. The previously described Y130L mutant version of UBE2M was employed to modify CUL1-RBX1 with the

I44A mutant version of NEDD8[39]. IKZF1 ZF2 (residues 141–169, with two point mutations K157R K165R and with a lysine added at position 140 to create a single target lysine at the N-terminus[57] was cloned with an N-terminal GST with a 3C-Prescission cleavage site and a non-cleavable C-terminal Strep-tag. IKZF1 ZF2 was purified by GST affinity chromatography, 3C-Prescission cleavage overnight, and size exclusion chromatography. UBE4B RING-like U-box domain (residues 1200-C-terminus) harboring D1268T N1271T point mutations that enhance activity[58] (hereafter referred to as UBE4B) was cloned with an N-terminal GST with TEV cleavage site. UBE4B was purified by GST affinity chromatography, TEV cleavage overnight, followed by ion exchange and size exclusion chromatography.

Peptides

All peptides were ordered >95% purity by HPLC.

Peptides used to quantify enzyme kinetics have the following sequences: IκBα– KERLLDDRHD(pS)GLD(pS)MRDEERRASY (obtained from New England Peptide)

β-catenin short– KSYLD(pS)GIH(pS)GATTAPRRASY (obtained from Max Planck Institute of Biochemistry Core Facility)

β-catenin medium– KAWQQQSYLD(pS)GIH(pS)GATTTAPRRASY (obtained from New England Peptide)

β-catenin long– KAAVSHWQQQSYLD(pS)GIH(pS)GATTAPRRASY (obtained from Max Planck Institute of Biochemistry Core Facility)

β-catenin for sortase-mediated transpeptidation to UB to generate a homogeneously UB-linked substrate – GGGGYLD(pS)GIH(pS)GATTAPRRASY (obtained from Max Planck Institute of Biochemistry Core Facility)

Peptides used for qualitative assays monitoring “substrate priming”, i.e. fluorescent UB transfer from UBE2D~UB to substrate, have the following sequences: IκBα– KKERLLDDRHD(pS)GLD(pS)MKDEE as described previously[41].

CyE– KAMLSEQNRASPLPSGLL(pT)PPQ(pS)GRRASY as described previously[41].

Non-modifiable substrate analog used in competition experiment in Extended data figure 3d has the following sequence: IκBα– RRERLLDDRHD(pS)GLD(pS)MRDEE (obtained from Max Planck Institute of Biochemistry Core Facility)

Peptides used in cryo EM experiments—For structure representing neddylated CRL1$^{\beta\text{-TRCP}}$-UBE2D~UB-IκBα substrate described in detail and cryo EM experiments shown in Extended data Figure 3e, f, h, i)

IκBα– CKKERLLDDRHD(pS)GLD(pS)MKDEEDYKDDDDK (obtained from Max Planck Institute of Biochemistry Core Facility)

For cryo EM reconstructions of unnneddylated and neddylated CRL1$^{β\text{-}TRCP}$-IκBα substrate shown in Extended data Figure 2a, b

IκBα– KKERLLDDRHD(pS)GLD(pS)MKDEE as described previously[41].

Enzyme kinetics

UBE2D3 titrations under substrate single encounter conditions for estimation of the K_m for E2 employed by neddylated CRL1—These experiments used full-length CRL1$^{β\text{-}TRCP2}$ and UBE2D3, referred to here as CRL1$^{β\text{-}TRCP}$ and UBE2D. 50 μM peptide substrate (for a list of peptides that were employed in the assay, please see the 'peptides used to quantify enzyme kinetics' section above) was radiolabeled with 5 kU of cAMP-dependent protein kinase (New England Biolabs) in the presence of [$γ^{32}$P]-ATP for 1 hour at 30°C. Two mixtures were prepared prior to initiation of the reaction: a UBA1/UB mix containing unlabeled substrate competitor peptide that was identical in sequence to the labeled one (the one exception being the UB-β-catenin substrate, where the unlabeled β-catenin for sortase peptide was used), and a neddylated or unneddylated (bearing a CUL1 K720R mutation to prevent low-level ubiquitylation by UBE2D[3]) CRL1$^{β\text{-}TRCP}$/labeled peptide substrate mix, The UBA1/UB mix contained reaction buffer composed of 30 mM Tris-HCl, 100 mM NaCl, 5 mM $MgCl_2$, 2 mM ATP, and 2 mM DTT pH 7.5. The UB concentration was 80 μM, the UBA1 was 1 μM, and the unlabeled peptide was 100 μM. UBE2D was first prepared as a 2-fold dilution series from a variable stock concentration, then introduced individually into tubes containing equal amounts of the UBA1/UB mix. The CRL1$^{β\text{-}TRCP}$/labeled peptide substrate mix contained the same reaction buffer as the UBA1/UB/UBE2D mix, 0.5 μM CRL1$^{β\text{-}TRCP}$, and 0.2 μM labeled peptide substrate. The reactions were initiated at 22°C by combining equal volumes of both mixes, rapidly vortexed, and quenched after 10 seconds in 2x SDS-PAGE buffer containing 100 mM Tris-HCl, 20% glycerol, 30 mM EDTA, 4% SDS, and 4% β-mercaptoethanol pH 6.8. Each titration series was performed in duplicate and resolved on hand-cast, reducing 18% SDS-PAGE gels. The gels were imaged on a Typhoon 9410 Imager and quantitation of substrate and products was performed using Image Quant (GE Healthcare). The product of each lane was measured as the fraction of the ubiquitylated products divided by the total signal, plotted against the UBE2D concentration, and fit to the Michaelis-Menten equation to estimate K_m (GraphPad Prism software). The standard error was calculated using Prism and has been provided in Table 1 for all estimates of K_m.

Estimating the rates of UB transfer to CRL1-bound substrate using pre-steady state kinetics.—These experiments used full-length CRL1$^{β\text{-}TRCP2}$ and UBE2D3, referred to here as CRL1$^{β\text{-}TRCP}$ and UBE2D, respectively. Separate UBA1/UBE2D/UB and CRL1$^{β\text{-}TRCP}$/labeled peptide substrate mixes were prepared to assemble single encounter ubiquitylation reactions. For most reactions, the UBA1/UBE2D3/UB mix contained reaction buffer, 80 μM UB, 1 μM UBA1, 40 μM UBE2D, and 200 μM unlabeled competitor substrate peptide. For all reactions containing either CUL1 K720R or reactions containing UBE2D

H32A assayed with wild-type neddylated CUL1, CUL1 modified with the I44A mutant NEDD8, or modified with UB R72A permitting ligation to CUL1, 120 μM UB and 70 μM UBE2D were used. The $CRL1^{\beta\text{-}TRCP}$/labeled peptide substrate mixes contained reaction buffer, 0.5 μM $CRL1^{\beta\text{-}TRCP}$, and 0.2 μM labeled peptide (for a list of peptides that were employed in the assay, please see the 'peptides used to quantify enzyme kinetics' section above). Each mix was separately loaded into the left or right sample loops on a KinTek RQF-3 quench flow instrument, and successive time points were taken at 22°C by combining the mixtures with drive buffer composed of 30 mM Tris-HCl and 100 mM NaCl pH 7.5. Reactions were quenched at various time points in 2x SDS-PAGE buffer to generate the time courses. Substrate and products from each time point were resolved on hand-cast, reducing 18% SDS-PAGE gels. The gels were imaged on a Typhoon 9410 Imager, and substrate and product bands were individually quantified as a percentage of the total signal for each time point using Image Quant (GE). Reactions were performed in duplicate, and the average of each substrate or product band was used for the analysis. The data for substrate (S0) or mono-ubiquitylated product (S1) bands were fit to their respective closed-form solutions as described[59] using Mathematica to obtain the values $k_{obs}^{S0\text{-}S1}$ and $k_{obs}^{S1\text{-}S2}$ (Extended Data Table 1). The standard errors were calculated in Mathematica and has been provided in Table 1 for all estimates of k_{obs}.

Multiturnover assays with short β-catenin.—Multiturnover assay showing the UB transfer to short β-catenin (Extended Data Figure 6c–d) was performed as above, but without the excess unlabeled β-catenin peptide substrate. Time points were collected by quenching in 2X SDS-PAGE loading buffer. Substrate and product were separated by SDS-PAGE followed by autoradiography. The fraction of unmodified substrate (S0) was quantified and fit to either a one phase decay (unneddylated) or linear (neddylated) models (Prism 8). Similarly, products containing 5 or more UBs were quantified and fit to either an exponential growth (neddylated) or linear (unneddylated) models. Experiments were performed in duplicate.

Generation of Ubiquitylated β-catenin fusion via Sortase reaction—A mimic of ubiquitylated β-catenin was generated by fusing a ubiquitin with a C-terminal LPETGG with a GGGG–β-catenin peptide. Reaction was incubated with concentrations of 50μM UB^{LPETGG}, 300μM GGGG-β-catenin peptide, and 10μM 6xHis-Sortase A for 10 minutes in 50 mM Tris 150 mM NaCl 10 mM $CaCl_2$ pH 8.0, removed Sortase A by retention on nickel resin, and further purified by size exclusion chromatography in 25 mM HEPES 150mM NaCl 1mM DTT pH 7.5.

Sequence of Ubiquitin with sortase motif:

MQIFVKTLTGKTITLEVEPSDTIENVKAKIQDKEGIPPDQQRLIFAGKQLEDGRTLSDY NIQKESTLHLVLRLRGSGSGSLPETGG

Other biochemical assays

For experiments comparing activity of neddylated with unneddylated CRLs or CUL-RBX1 complexes, in the unneddylated versions the NEDD8 modification sites of CUL1 and CUL4 were mutated to Arg (CUL1 K720R and CUL4A K705R) to prevent obscuring interpretation

of the results by low-level ubiquitylation of the NEDD8 consensus Lys during the ubiquitylation reactions[3].

Substrate priming assays—Experiments in Extended Data Fig 8a–f used full-length CRL1$^{\beta\text{-TRCP2}}$ and UBE2D3. Ubiquitylation of IκBα by CRL1$^{\beta\text{-TRCP}}$ via UBE2D3 was monitored using a pulse-chase format that specifically detects CRL$^{\beta\text{-TRCP}}$-dependent UB modification from UBE2D to IκBα independently of effects on UBA1-dependent formation of the UBE23D~UB intermediate. The pulse reaction generated a thioester linked UBE2D~UB intermediate and contained 10 μM UBE2D, 15 μM fluorescent UB, 0.2 μM UBA1 in 50 mM Tris, 50 mM NaCl, 2.5 mM $MgCl_2$, 1.5 mM ATP pH 7.5 incubated at room temperature for 10 minutes. The pulse reaction was quenched with 50 mM EDTA on ice for 5 minutes, then further diluted to 100 nM UBE2D in 25 mM MES, 150 mM NaCl pH 6.5 for subsequent mixture with components of the reaction for neddylated CRL1$^{\beta\text{-TRCP}}$-dependent UB transfer to the substrate in the chase reaction. The chase reaction mix consisted of 400 nM CRL (NEDD8-CUL1-RBX1-SKP1-β-TRCP), and 1μM substrate (phosphorylated peptide derived from IκBα) in 25 mM MES, 150 mM NaCl pH 6.5 incubated on ice. After the quench, the pulse reaction mix was combined with the chase reaction mix at a 1:1 ratio on ice. The final reaction concentrations were 50 nM UBE2D (in thioester-linked UBE2D~UB complex) and 200 nM neddylated CRL1$^{\beta\text{-TRCP}}$ to catalyze substrate ubiquitylation. Samples were taken each time point, quenched with 2X SDS-PAGE sample buffer, protein components were separated on non-reducing SDS-PAGE, and the gel was scanned on a Amersham Typhoon (GE).

Substrate priming reactions assaying effects of variations in UBE2D shown in Extended Data Figure 8g–i on CRL1^{FBW7}-dependent ubiquitylation a phosphopeptide derived from CyE were performed similarly as those for CRL1$^{\beta\text{-TRCP}}$ described above with 100 nM UBE2D~UB (based on concentration of UBE2D from the pulse reaction), 500 nM neddylated CUL1-RBX1-SKP1-FBW7 (residues 263 to the C-terminus), and 2.5 μM CyE phosphopeptide in 25 mM HEPES 150 mM NaCl pH 7.5 at room temperature. Experiments testing effects of variations in NEDD8 (or its substitution with UB R72A) were performed in the same manner, except with 250 nM NEDD8 (or variant)-modified CUL1-RBX1-SKP1-FBW7 (residues 263 to the C-terminus).

Our assay for CRL4^{CRBN} ubiquitylation of IKZF was established based on findings that ZF2 mediates tight immunomodulatory-drug dependent interaction sufficient to target degradation, UBE2D3 contributes to stability of CRL4^{CRBN} neomorphic substrates in cells[57,60,61]. Substrate priming reactions showing controls and assaying effects of variations in NEDD8 and UBE2D3 shown in Extended Data Figure 8j–o monitored ubiquitylation of IKZF ZF2 with 400 nM UBE2D~UB (concentration determined by that of UBE2D in the chase reaction), 500 nM NEDD8-CUL4-RBX1-DDB1-CRBN, 5 μM Pomalidomide, and 2.5 μM IKZF ZF2 in 25 mM HEPES, 150 mM NaCl pH 7.5 at room temperature. Effects of swapping NEDD8 for UB (R72A) on CRL4^{CRBN} ubiquitylation of IKZF ZF2 shown in Extended Data Figure 8m were performed similarly but with 100 nM UBE2D~UB, 250 nM NEDD8 or UB-modified CUL4-RBX1-DDB1-CRBN, 2.5 μM Pomalidomide, and 1.25 μM IKZF ZF2.

Assays for intrinsic activation of UBE2D~UB intermediate—Assays shown in Extended Data Figure 3b, 3g and 7d–f, monitoring neddylated CUL1-RBX1 activation of the thioester-linked UBE2D~UB intermediate (i.e., in the absence of substrate) used the RBX1 N98R variant that is hyperactive toward UBE2D~UB[39]. Experiments in Extended Data Figures 3b, 3g and 7f were performed in pulse-chase format similar to substrate priming assays, but with 9 μM UBE2D~UB (loading reaction with 20 μM UBE2D, 30 μM UB and 0.5 μM UBA1), 500 nM E3 and 5 mM free lysine. For unneddylated CUL1-RBX1- or UBE4B-dependent discharge, 50 mM free lysine was used instead. Discharge assays shown in Extended Data Figure 7d and e used 5 μM UBE2D~UB (loading reaction with 20 μM UBE2D, 20 μM UB, and 0.5 μM UBA1), 500 nM E3, and 10 mM free lysine for neddylated CUL1-RBX1 dependent discharge, and 50 mM free lysine for unneddylated CUL1-RBX1 dependent discharge. All assays were visualized by Coommassie-stained SDS-PAGE.

Generation of a stable proxy for the UBE2D~UB-substrate intermediate

Preparation of His-TEV-UB(1–75)-MESNa—His-TEV-UB(1–75) was cloned using the method of Gibson[62] into pTXB1 (New England BioLabs) and transformed into BL21(DE3) RIL. Cells were grown in terrific broth at 37°C to OD_{600} = 0.8 and then induced with IPTG (0.5 mM), shaking overnight at 16°C. The harvested cells were resuspended (20 mM HEPES, 50 mM NaOAc, 100 mM NaCl, 2.5 mM PMSF pH 6.8), sonicated, and then centrifuged (20k RPM, 4°C, 30 min). Ni-NTA resin (1 mL resin per liter of broth, Sigma Aldrich) was equilibrated with the resuspension buffer and incubated with the cleared lysate at 4°C on a roller (30 RPM) for 1 hour. The resin was then transferred to a gravity column and washed (5 × 1 column volume with 20 mM HEPES, 50 mM NaOAc, 100 mM NaCl pH 6.8). Protein was then eluted (5 × 1 column volume with 20 mM HEPES, 50 mM NaOAc, 100 mM NaCl 300 mM Imidazole pH 6.8). Ubiquitin was then cleaved from the chitin binding domain by diluting the eluted protein 10:1 (v/v) with 20 mM HEPES, 50 mM NaOAc, 100 mM NaCl, 100 mM sodium 2-mercaptoethanesulfonate (Sigma Aldrich) pH 6.8. This solution was incubated at room temperature overnight on a roller (30 RPM). UB-MESNa was finally purified by size-exclusion chromatography (SD75 HiLoad, GE Healthcare) equilibrated with 12.5 mM HEPES, 25 mM NaCl pH 6.5.

Sequence of His-TEV-UB(1–75)-chitin binding domain:

MGSSHHHHHHENLYFQGSGGMQIFVKTLTGKTITLEVEPSDTIENVKAKIQD

KEGIPPDQQRLIFAGKQLEDGRTLSDYNIQKESTLHLVLRLRGCFAKGTNVL

MADGSIECIENIEVGNKVMGKDGRPREVIKLPRGRETMYSVVQKSQHRAH

KSDSSREVPELLKFTCNATHELVVRTPRSVRRLSRTIKGVEYFEVITFEMGQ

KKAPDG

Native chemical ligation to make UB(1–75)-Cys-IκBα—His-UB(1–75)-MESNa (200 μM final concentration) and freshly dissolved IκBα peptide (H-CKKERLLDDRHDpSGLDpSMKDEEDYKDDDDK-OH) (1000 μM final concentration)

were combined in a 1.5 ml tube in 50 mM $NaPO_4$, 50 mM NaCl pH 6.5. This was incubated with rocking at 30 RPM for 1 h at room temperature before TCEP was added to 1 mM. After rocking for an additional hour at room temperature, the reaction was quenched by adding 500 mM $NaPO_4$ pH 8.0 to 45 mM. The entire solution was then incubated with Ni-NTA resin (300 μL for a 1 mL reaction) at 30 RPM for 1 h at 4°C. In a gravity column, the resin was then washed 6 × 300 μL with 50 mM $NaPO_4$, 50 mM NaCl, 1 mM β-mercaptoethanol pH 8.0. Protein was eluted with 50 mM $NaPO_4$, 50 mM NaCl, 1 mM β-mercaptoethanol, 300 mM imidazole pH 8.0. Fractions were analyzed by SDS-PAGE and nanodrop.

Formation of disulfide between UBE2D Cys85 and UB(1–75)-Cys-IκBα—The same approach was used to generate complexes for UBE2D2 and UBE2D3, referred to collectively as UBE2D. UBE2D C21I C107A C111D was purified from size exclusion chromatography (see above) and then immediately used without freezing. After SEC, the protein was concentrated (Amicon, EMD Milipore) to 600 μM. 2 × 100 μL of protein were separately desalted (2 × Zeba, 0.5 mL column, 7K MWCO, ThermoFisher) to 20 mM HEPES, 250 mM NaCl, 5 mM EDTA pH 7.0. Elutions were combined and immediately added together to 34 μL 10 mM 5,5'-dithiobis-(2-Nitrobenzoic acid) (SigmaAldrich, dissolved in 50 mM $NaPO_4$ pH 7.5) and mixed by pipetting before incubating at room temperature for 30 min. The solution was then desalted (2 × Zeba, 0.5 mL column, 7K MWCO, ThermoFisher) to 20 mM HEPES, 250 mM NaCl, 5 mM EDTA pH 7.0 at the same time that UB(1–75)_Cys_IκBα (500 μL at 100 μM) was desalted (1 × Zeba, 2 mL column, 7K MWCO, ThermoFisher) to the same buffer. The UBE2D and UB components were then immediately combined and incubated at room temperature for 30 min, at which point, the sample was loaded to a Superdex 75 Increase column (GE Healthcare) equilibrated with 20 mM HEPES, 250 mM NaCl, 5 mM EDTA pH 7.0.

Comparing ability of stable proxy for the UBE2D~UB-substrate intermediate and subcomplexes to compete with ubiquitylation—Assays comparing ubiquitylation in the presence of competitors (stable proxy for the UBE2D~UB-substrate intermediate, stable isopeptide-linked mimic of UBE2D~UB, and nonmodifiable substrate peptide) were carried out similarly as described for our substrate priming assay described below with the following modifications. The assay was performed in pulse-chase format to exclude potential for competitors to impact generation of the UBE2D~UB intermediate. In the pulse reaction, a thioester linked UBE2D~UB intermediate was generated by incubating 10 μM UBE2D, 15 μM fluorescent UB, and 0.2μM UBA1 in a buffer that contained 50 mM Tris, 50 mM NaCl, 2.5 mM $MgCl_2$, and 1.5 mM ATP pH 7.6 at room temperature for 10 minutes. The pulse reaction was next quenched by the addition of an equal volume of 50 mM Tris, 50 mM NaCl, 100 mM EDTA pH 7.6 and placed on ice for 5 minutes, then further diluted to 100 nM in a buffer containing 25 mM MES pH 6.5 and 150 mM NaCl. The E3-substrate mix consisted of 400 nM NEDD8-CUL1-RBX1, 400 nM SKP1-β-TRCP, 1 μM IκBα peptide, with or without 1 μM competitor in a buffer consisting of 25 mM MES and 150 mM NaCl pH 6.5, and was incubated at 4°C for 10 minutes to achieve equilibrium. Reactions were initiated on ice by the addition of an equal volume of pulse reaction to the E3-substrate mix, resulting in final reaction conditions that were 50 nM UBE2D~UB, 200 nM E3 neddylated $CRL1^{\beta\text{-}TRCP}$, and 500 nM substrate with or without 500nM competitor.

Samples were taken at the indicated time points and quenched with 2X. SDS-PAGE sample buffer. Substrate and products were then separated by SDS-PAGE, and subsequently visualized using an Amersham Typhoon (GE).

Early attempt to visualize UB transfer by neddylated CRL1$^{\beta\text{-TRCP}}$ and UBE2D and rationale for approaches to improve EM samples—In our initial attempt to determine a structure visualizing UB transfer by neddylated CRL1$^{\beta\text{-TRCP}}$ and UBE2D, we employed a full-length β-TRCP (β-TRCP2), which is a homodimer[27] and a proxy for a UBE2D~UB-substrate intermediate based on a method used to capture a Sumoylation intermediate[63]. In the prior study, SUMO was installed via an isopeptide bond on a residue adjacent to the E2 catalytic Cys, and substrate was crosslinked to the E2 Cys via an ethanedithiol linker. Here, we introduced the corresponding lysine substitution in the background of an optimized E2 (UBE2D2 L119K, C21I, C107A, C111D). Using high concentrations of UBA1 and high pH, we generated an isopeptide-bonded complex between UB and this UBE2D2 variant in a manner dependent on the L119K mutation, and crosslinked the Cys of the IκBα substrate mimic peptide to the UBE2D~UB complex using EDT as described[63]. The resultant cryo EM data map, shown in Extended Data Figure 3e, presented two major challenges. First, the dimer exacerbated structural heterogeneity, with minor differences presumably based on natural motions between the two protomers. Second, the donor UB was poorly visible, presumably due to not being linked to the catalytic Cys. Thus, we generated many samples in parallel to overcome these challenges by (1) using a monomeric version of β-TRCP1 that had been previously crystallized[20], (2) removing two loops in SKP1 that are known to be flexible and not required for ubiquitylation activity (although they are required for CAND1-mediated substrate-receptor exchange)[13,54], (3) devising a chemical approach to synthesize a proxy for the UBE2D~UB-substrate intermediate where all three entities are simultaneously linked to the E2 catalytic Cys, (4) using a point mutant version of RBX1 that is hyperactive for substrate priming with UBE2D but defective for UB chain elongation with UBE2R-family E2s[39]. Notably, with a K_m for UBE2D3 of 350 nM and rates of ubiquitylating the medium β-catenin peptide substrate of 8.9 sec^{-1} (S0-S1) and 0.25 sec^{-1} (S1-S2), we confirmed that the monomeric version of neddylated CRL1$^{\beta\text{-TRCP1}}$ is kinetically indistinguishable from full-length, homodimeric neddylated CRL1$^{\beta\text{-TRCP2}}$.

Cryo-EM

Sample preparation—For neddylated or unneddylated CUL1-RBX1-SKP1-β-TRCP-IκBα samples, subcomplexes were mixed with equimolar ratio with 1.5 excess substrate peptide, incubated for 30 minutes on ice, and purified by size exclusion chromatography in 25 mM HEPES, 150 mM NaCl, 1 mM DTT pH 7.5. The complex was further concentrated and crosslinked by GraFix[64]. The sample was next liberated of glycerol using Zeba Desalt Spin Columns (ThermoFisher), concentrated to 0.3mg/ml, and 3μL of sample was applied Quantifoil R1.2/1.3 holey carbon grids (Quantifoil) and was plunged frozen by Vitrobot Mark IV in liquid ethane. Structure determination of the neddylated CUL1-RBX1-SKP1-β-TRCP-UB~UBE2D-IκBα complex used a similar method as above, with 1.5-fold excess of the stable proxy for the UBE2D~UB-IκBα intermediate, but with no DTT in buffer. After SEC, GraFix, and desalting, 3μL of 0.08mg/ml sample was applied to graphene oxide coated

Quantifoil R2/1 holey carbon grids (Quantifoil)[65] and was plunged frozen by Vitrobot Mark IV in liquid ethane.

Electron microscopy—Datasets were collected on a Glacios at 200kV using a K2 Summit direct detector in counting mode. For the dataset of CUL1-RBX1-SKP1-β-TRCP1ΔD-IκBα, 6433 images were recorded at 1.181Å/pixel with a nominal magnification of 36,000x. A total dose of 60 $e^{-}/Å^2$ were fractionated over 50 frames, with a defocus range of −1.2μm to −3.3μm. For NEDD8-CUL1-RBX1-SKP1-β-TRCP1ΔD-IκBα, 2061 images were recorded at 1.885Å/pixel with a nominal magnification of 22,000x. Total dose of 59 $e^{-}/Å^2$ were fractionated over 38 frames, with a defocus range of −1.2μm to −3.3μm.

Datasets were also collected on a Talos Arctica at 200kV using a Falcon II direct detector in linear mode. For each sample, around 800 images were recorded at 1.997Å/pixel with a nominal magnification of 73,000x. A total dose of ~60 $e^{-}/Å^2$ were fractionated over 40 frames, with a defocus range of −1.5μm to −3.5μm.

High resolution cryo-EM data were collected on a Titan Krios electron microscope at 300kV with a Quantum-LS energy filter, using a K2 Summit direct detector in counting mode. 9112 images were recorded at 1.06Å/pixel with a nominal magnification of 130,000x. A total dose of 70.2 $e^{-}/Å^2$ were fractionated over 60 frames, with a defocus range of −1.2μm to −3.6μm.

Data processing—Frames were motion-corrected using RELION-3.0[66] with dose weighting. CTF was estimated using CTFFIND[67]. Particles were picked with Gautomatch (K. Zhang, MRC Laboratory of Molecular Biology, Cambridge). 2D classification was performed in RELION-3.0, followed by 3D ab initio model building by sxviper.py from SPARX[68]. The initial model from sxviper.py was imported to RELION-3.0 for further 3D classification, refinement, post-processing, and particle polishing using frames 2–25.

Protein identification and model building—The final reconstructions displayed clear main chain and side chain densities, that enabled us to model and refine the atomic coordinates. Known components (CUL1-RBX1 PDB ID 1LDJ and 4P5O, SKP1ΔΔ-β-TRCP1 PDB ID 1P22, UBE2D~UB with a backside-bound UB to be replaced by NEDD8 sequences PDB ID 4V3L) were manually placed as a whole or in parts and fit with rigid body refinement using USCF Chimera[69]. The resultant complete structure underwent rigid body refinements in which each protein/domain were allowed to move independently. Further iterative manual model building and real space refinements were carried out until good geometry and map to model correlation was reached. Manual model building and rebuilding were done using COOT[70] and Phenix.refine[71] was used for real space refinement.

Data Availability Statement

The atomic coordinates and EM maps have been deposited in the RCSB with accession code PDB ID 6TTU and EMDB with codes EMD-10585, EMDB-10578, EMDB-10579, EMDB-10580, EMDB-10581, EMDB-10582, EMDB-10583. Uncropped gel source data are included as supplementary information. All other reagents and data (e.g. raw gels of replicate experiments and raw movie EM data) are available from the corresponding author upon request.

Extended Data

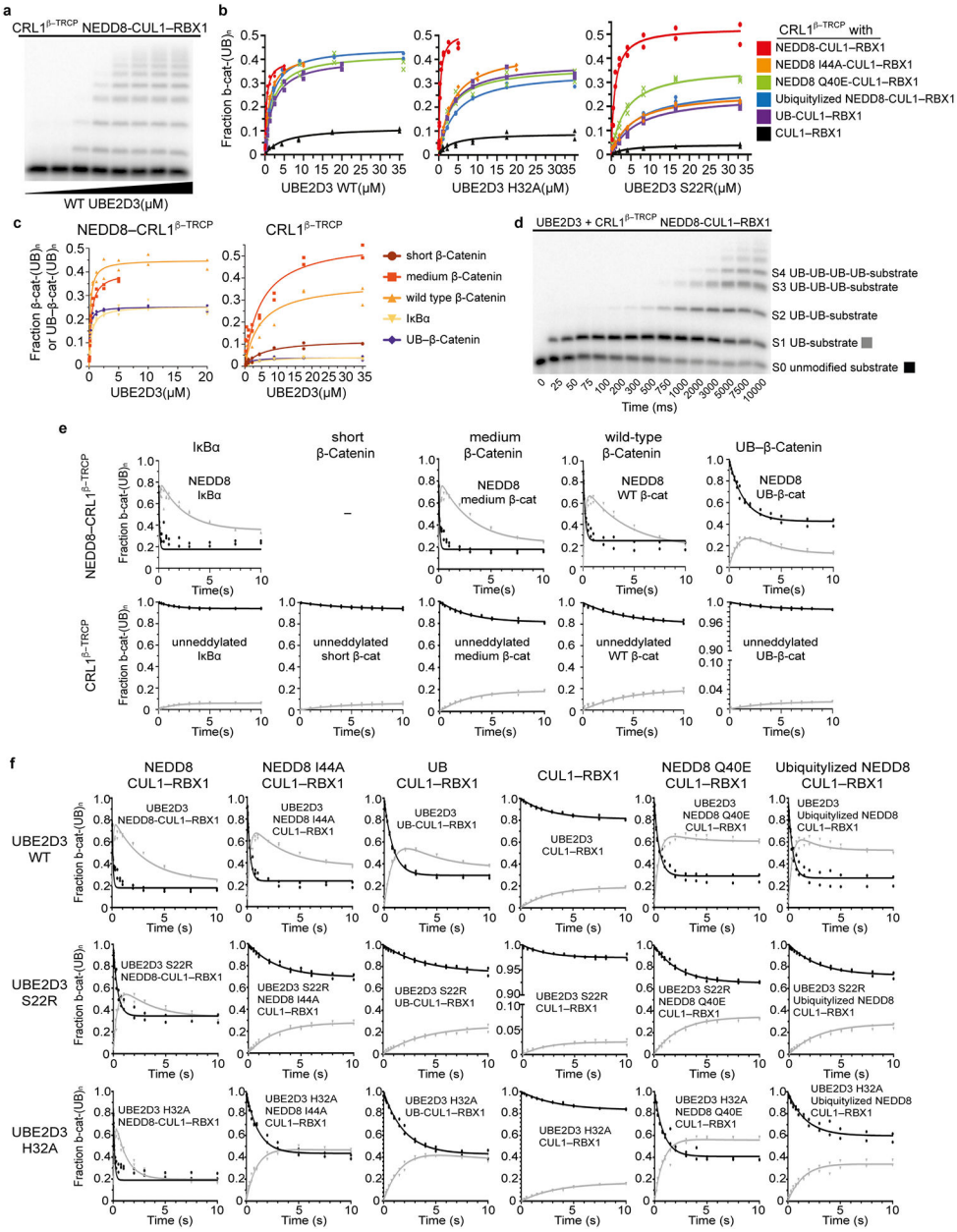

Extended Data Figure 1 |. Quantitative pre-steady state enzyme kinetics of neddylated CRL1$^{β\text{-}TRCP}$- and UBE2D-dependent ubiquitylation.

Gel images are representative of independent technical replicates (n=2); The symbols from graphs show the data from independent experiments (n = 2). **a**, Autoradiogram of SDS-PAGE gel showing products of ubiquitylation reactions under single encounter conditions for interaction of radiolabeled substrate ("medium β-catenin" substrate peptide derived from β-catenin) with neddylated CRL1$^{β\text{-}TRCP}$, titrating UBE2D3 (referred to as UBE2D hereafter in legend). Each lane represented a single ubiquitylation reaction that was used to estimate the fraction of peptide that had been converted into ubiquitylated products as a function of UBE2D concentration. **b**, Plots of the fraction of substrate that had been converted to ubiquitylated products versus UBE2D concentration for ubiquitylation reactions containing

either WT (as shown in **a**) or UBE2D S22R or H32A mutants. Various CRL1$^{\beta\text{-TRCP}}$ complexes were assayed that contained either WT neddylated CRL1$^{\beta\text{-TRCP}}$ (red), CRL1$^{\beta\text{-TRCP}}$ complexes modified by NEDD8 variants harboring I44A (orange), Q40E (green), "Ubiquitylizing" (L2Q K4F E14T D16E G63K G64E) substitutions (blue), CRL1$^{\beta\text{-TRCP}}$ modified by UB R72A that is competent for ligation to CUL1 (purple), or unmodified CRL1$^{\beta\text{-TRCP}}$ (CUL1 with the neddylation site K720R mutation, black). Duplicate data points from independent experiments performed with identical samples are shown and were fit to the Michaelis-Menten model to estimate the K_m of UBE2D for CRL1$^{\beta\text{-TRCP}}$ using non-linear curve fitting (GraphPad Prism). **c**, Plots of the fraction of substrate that had been converted to ubiquitylated products versus UBE2D concentration for ubiquitylation reactions with various substrate peptides: derived from IκBα (but with a single acceptor Lys); derived from β-catenin; derived from β-catenin with different spacing between the phosphodegron motif and a potential acceptor Lys (a "medium β-catenin" substrate peptide with a 9-residue spacer between the β-catenin phosphodegron and acceptor matching the relative position of these moieties in IκBα, and "short β-catenin" substrate wherein the four residues between these moieties are too few to bridge the structurally-observed gap between the substrate receptor and UBE2D~UB active site); and a homogeneous UB linked-β-catenin generated by sortase-mediated transpeptidation wherein the only lysines are from UB. **d**, Autoradiogram of SDS-PAGE gel showing results from rapid quench-flow reactions under pre-steady state single encounter conditions for interaction of radiolabeled substrate (a "medium β-catenin" phosphopeptide) with CRL1$^{\beta\text{-TRCP}}$. The representative raw data are from a reaction using WT UBE2D and WT neddylated CRL1$^{\beta\text{-TRCP}}$ and show time-resolved conjugation of increasing numbers of individual UB molecules. S0 = substrate with 0 UBs, S1 = substrate with 1 UB, S2 = substrate with 2 UBs, etc. **e**, Plots comparing various substrate peptides described in **c**, showing disappearance of unmodified substrate (S0) with black circles, and the appearance of mono-ubiquitylated substrate (S1) with gray triangles, in rapid quench-flow reactions all performed as in **d** and under single encounter conditions as in **a**. Duplicate data points from independent experiments performed with identical samples are shown. The data were fit to closed form equations (Mathematica) as previously described[59] to obtain both the rates for the transfer of the first UB to substrate ($k_{obs}^{S0\text{-}S1}$) and of the second UB to the singly UB-modified substrate ($k_{obs}^{S1\text{-}S2}$) as well as their associated standard error (Table 1). **f**, Plots from experiments performed and analyzed as described in **e**, except with radiolabeled "medium β-catenin" peptide substrate, CRL1$^{\beta\text{-TRCP}}$ variants containing the indicated versions of CUL1-RBX1, and with either WT or indicated mutant versions of UBE2D.

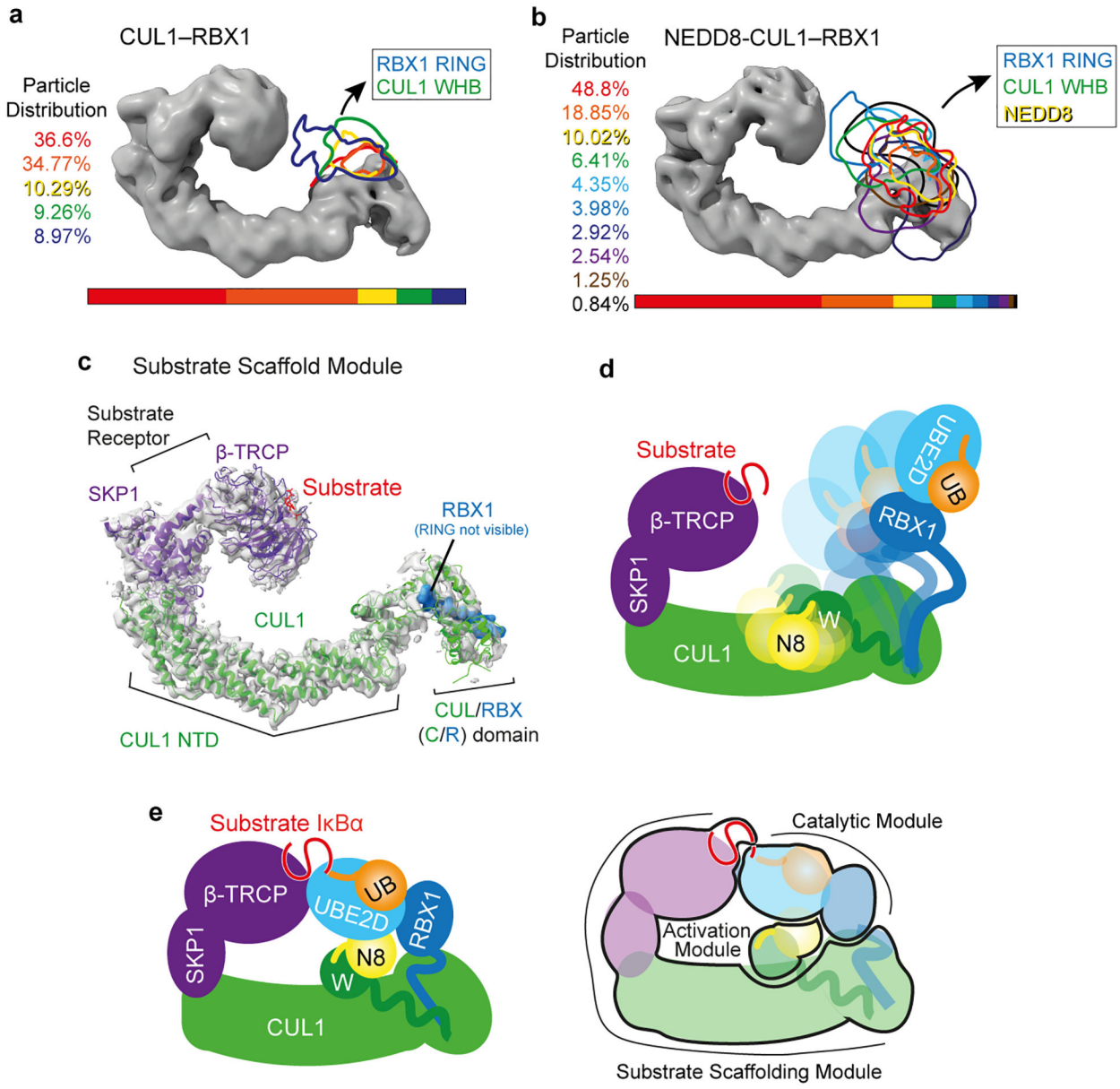

Extended Data Figure 2 |. CRL1$^{β\text{-}TRCP}$ RBX1 RING and CUL1 WHB domains, without or with a covalently-linked NEDD8, are dynamic in the absence of other factors and are harnessed in catalytic architecture for substrate ubiquitylation with UBE2D.

a, Cryo EM density corresponding to substrate scaffolding regions of unneddylated CRL1$^{β\text{-}TRCP}$ is shown as surface with that encompassing RBX1's RING and CUL1's WHB domains, outlined for different 3D classes in different colors corresponding to percent of particles in that 3D class. **b**, same as in **a**, but with neddylated CRL1$^{β\text{-}TRCP}$, with its surfaces outlined in different classes encompassing RBX1's RING, CUL1's WHB domain, and covalently modified NEDD8. **c**, Refined cryo EM density from CRL1$^{β\text{-}TRCP}$ reveals substrate scaffolding module bridging the substrate recruited to substrate receptor β-TRCP with the intermolecular cullin-RBX (C/R) domain, readily fitted with crystal structures of SKP1-β-TRCP [PDB: 1P22][20] and CUL1's N-terminal domain and the C/R domain of

CUL1-RBX1 [PDB: 1LDK][7]. **d**, Cartoon showing dynamics of NEDD8, its linked CUL1 WHB domain, and the RBX1 RING domain based on cryo EM data in **b** for substrate-bound neddylated $CRL1^{\beta\text{-}TRCP}$, and model for varying locations of the RBX1 RING-bound UBE2D~UB relative to the substrate awaiting ubiquitylation. **e**, Left, cartoon representation of the catalytic architecture based on the cryo EM data shown in Figure 2, representing neddylated $CRL1^{\beta\text{-}TRCP}$-catalyzed UB transfer from E2 UBE2D to an IκBα-derived substrate peptide. Right, semi-transparent version of the cartoon, highlighting the three modules (substrate scaffolding, catalytic, and activation modules), their constituents and locations establishing the catalytic architecture for substrate priming by neddylated $CRL1^{\beta\text{-}TRCP}$ and UBE2D.

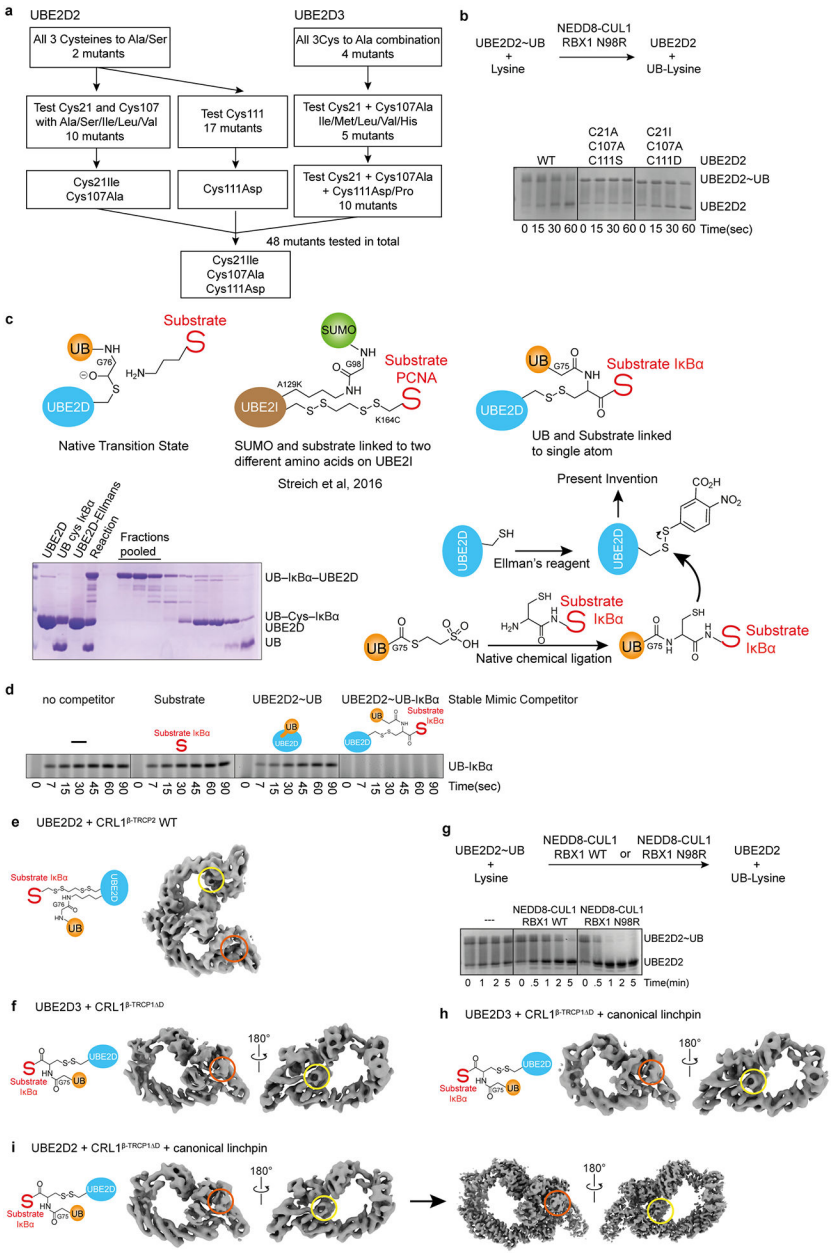

Extended Data Figure 3 |. Generation of stable proxy for UBE2D~UB-substrate intermediate, and characterization in complexes with neddylated CRL1$^{β\text{-}TRCP}$ by cryo EM and biochemistry.

Gel panels in this figure are representative from two independent experiments; n=2.

a, Our strategy for trapping a mimic of the transient neddylated CRL E2~UB-substrate complex requires that the E2 UBE2D contain only a single cysteine at the active site. However, UBE2D contains three additional cysteines (Cys21, Cys107, Cys111). Standard Cys replacements by Ser or Ala severely compromised activity. Based on the structural locations of these cysteines, we presumed that their mutation hindered formation of the RING-activated, closed, active UBE2D~UB conformation[28–30]. We thus devised a systematic structure- and random-based approach to identify suitable replacements that qualitatively maintain wild-type levels of activity with neddylated CRLs. Structural analysis

showed that Cys21 and Cys107 are in close proximity, such that mutation of both residues to Ala may generate a destabilizing cavity at this site. Combining UBE2D2 C107A with Cys21 mutated to Ile, Leu or Val to compensate for the reduced hydrophobic volume led to the identification of C21I C107A as a suitable version for testing of all other possible replacements for Cys111. A similar approach was taken for UBE2D3. A total of 48 different versions of UBE2D were tested to identify the C21I C107A C111D mutant for chemical trapping at the remaining active site Cys. **b**, Top, schematic of pulse-chase assay testing intrinsic activation of thioester-linked UBE2D~UB intermediates. Although this is often tested by monitoring RING-dependent discharge of UB from UBE2D to free lysine, RBX1 RING-dependent activity is limited in this assay due to sequence constraints imposed by the requirements for binding to partners other than UBE2D[39]. Nonetheless, substrate-independent activation of UBE2D~UB can be readily visualized using CUL1 complexed with a previously-described hyperactive RBX1 N98R mutant[39], and high enzyme and lysine concentrations. UBE2D~UB generated in a pulse reaction was mixed with NEDD8-modified CUL1-RBX1 (shown here with N98R mutant) and free lysine, and UB discharge was monitored over time by Coomassie-stained SDS-PAGE as shown in representative gel on bottom demonstrating that standard Ser/Ala mutations of noncatalytic cysteines compromised activity (shown for C21A C107A C111S), while optimized version (C21I C107A C111D) retains wild-type like activity. **c**, Overview of the generation of our stable proxy for the phosphorylated IκBα substrate intermediate linked at a single atom, and comparison to the prior method employed to visualize non-canonical Lys sumoylation[63]. **d**, Experiment validating our stable proxy for the UBE2D~UB-phosphorylated IκBα substrate intermediate linked at a single atom, based on the hypothesis that its simultaneous occupation of the binding sites for the UBE2D~UB intermediate and substrate should result in more potent inhibition of a neddylated CRL1$^{\beta\text{-TRCP}}$-dependent substrate priming reaction compared to the individual constituents of the complex. **e**, Cryo EM reconstruction of neddylated CRL1$^{\beta\text{-TRCP2}}$ (with full-length, dimeric β-TRCP2) bound to a mimic of the UBE2D2~UB-IκBα generated by adapting the method used previously to visualize non-canonical Lys sumoylation[63], where UB is isopeptide-bonded to a UBE2D L119K residue substitution, and a substrate Cys replacement for the acceptor is disulfide-bonded to the UBE2D2 catalytic Cys. This EM map visualizes the catalytic architecture of dimeric CRL1$^{\beta\text{-TRCP2}}$ wherein the dimerization domain agrees well with the prior crystal structure[27], and its linked NEDD8 (encircled in yellow) is bound to the backside of UBE2D, but the donor UB (absent from region circled in orange) was not visible, presumably due to inadequacies of the method used to generate this mimic of the catalytic intermediate, in which the UB and substrate are not both simultaneously linked to the UBE2D catalytic Cys. Variations between the two protomers of the dimer also exacerbated sample heterogeneity. **f**, Cryo EM reconstruction of neddylated CRL1$^{\beta\text{-TRCP1}\Delta\text{D}}$ (with monomeric version of β-TRCP1, from residue 175 to the C-terminus[20]) bound to our newly devised proxy for the UBE2D3~UB-IκBα intermediate. The phoshpo-IκBα peptide-substrate-bound β-TRCP-SKP1-CUL1-RBX1-NEDD8-UBE2D portion of this map superimposes with the map for the dimeric complex shown in **e**, but here the entire complex is visible, including both the NEDD8 (encircled in yellow) and donor UB (encircled in orange). **g**, To further increase cryo EM sample homogeneity, we considered that the RBX1 RING sequence represents a compromise to meet requirements for its many different catalytic activities achieved with

neddylation E2s, various UB carrying enzymes, and regulators including the inhibitor GLMN[72]. Therefore, we mutationally introduced a second RBX1 linchpin residue (N98R) previously shown to improve neddylated CRL and UBE2D-dependent substrate priming at the expense of other RBX1-dependent functions (e.g. with UBE2M and UBE2R2)[39]. Shown is a Coommassie-stained SDS-PAGE gel from assay for intrinsic activity of UBE2D~UB, showing enhanced neddylated CRL-dependent activation of discharge to free lysine with the RBX1 N98R mutation. **h**,**i**, Cryo EM reconstructions of neddylated CRL1$^{\beta\text{-TRCP1}\Delta D}$ with RBX1 N98R bound to our newly devised proxies for the UBE2D3~UB-IκBα and UBE2D2~UB-IκBα intermediates, the latter of which was pursued for high resolution electron microscopy (final reconstruction refined to 3.7Å resolution shown on right).

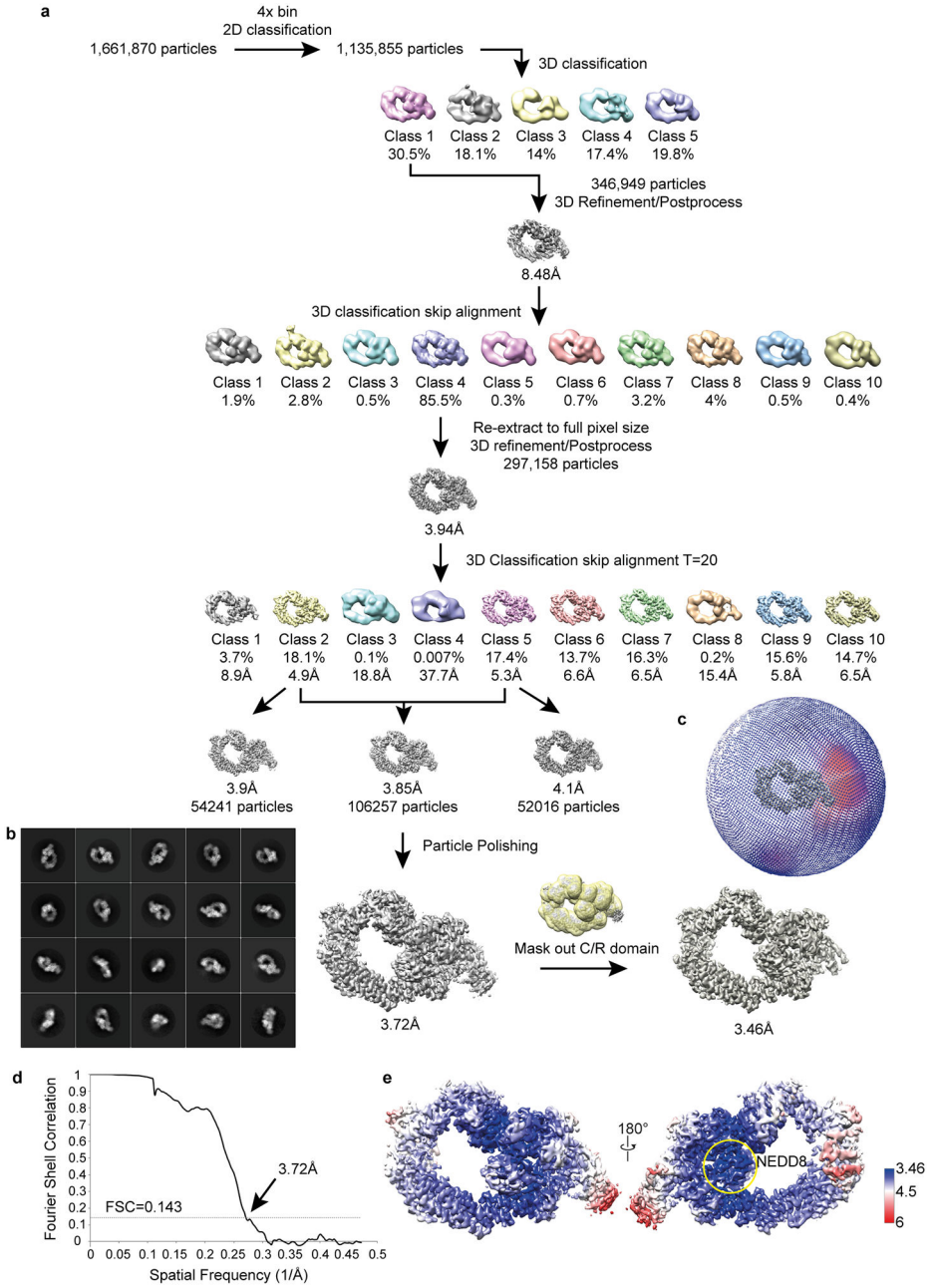

Extended Data Figure 4 |. Cryo-EM image processing flow chart.

a, Cryo-EM image processing work chart. Ultimately, reconstruction of the data yielded a focused refinement at 3.46 Å resolution and a global refinement at 3.7 Å resolution that superimposes well with lower resolution maps obtained during attempts to visualize substrate priming with neddylated wild-type dimeric CRL1$^{\beta\text{-TRCP}}$. **b**, 2D classes representing particles used for final reconstructions. **c**, Angular distribution of final reconstruction. **d**, Gold standard Fourier Shell Correlation curve showing overall resolution at 3.72Å at FSC=0.143. **e**, EM density map colored by local resolution. NEDD8, encircled in yellow, is the entity displaying the highest local resolution in the map.

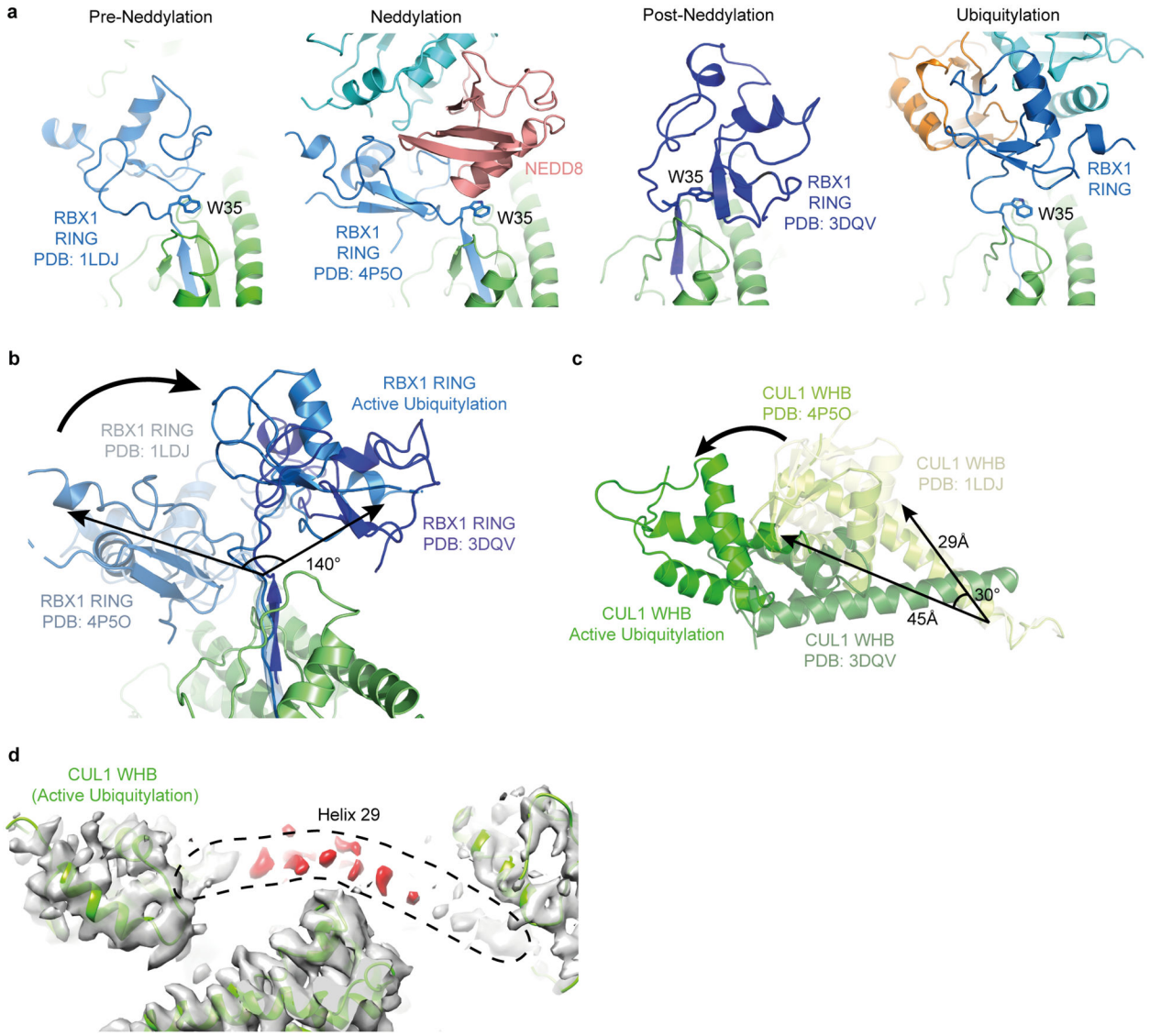

Extended Data Figure 5 |. Extraordinary cullin-RING conformational changes in catalytic architecture juxtaposing substrate and ubiquitylation active site.

a, Side-by-side comparison of relative RING domain locations in different CRL complexes after superposition of the C/R domains from the original CUL1-RBX1 structure (PDB ID 1LDJ, "Pre-Neddylation", which data herein shows is dynamic, although the crystal structure likely captured the conformation allowing CAND1 binding and substrate receptor exchange)[7], the structure representing the Neddylation reaction (PDB ID 4P5O)[39], and a structure of a neddylated CUL5-RBX1 domain (PDB ID 3DQV, labeled "Post-Neddylation", which revealed potential for neddylated CUL WHB and RBX1 RING domain conformational changes[3], and data herein shows is dynamic), and the structure presented here showing how the neddylated CUL1 WHB domain and RBX1 RING are harnessed in a catalytic architecture for "Active ubiquitylation". RBX1's Trp35 is highlighted to show it serving as a multifunctional platform for either the RING domain in different orientations, or for the E2-linked NEDD8 during neddylation[39]. **b**, Superposition of the structures shown in

a, highlighting different relative RING positions. **c**, Comparison of CUL WHB domain relative locations after superimposing their C/R domains (not shown). **d**, Cryo EM density from the neddylated CRL1$^{\beta\text{-TRCP}}$-UBE2D~UB-substrate intermediate complex, showing patchiness of region corresponding to CUL1 "Helix-29"[7]. This CUL1 region connecting the C/R and WHB domains is visible only as patchy density, whereas in prior cullin crystals this forms the rod-like Helix-29 continuing into the WHB domain[7]. It seems CUL1's Helix-29 dissolves into a flexible tether, which rationalizes the previously observed proteolytic sensitivity of this region in a neddylated CUL1-RBX1 complex[3], and enables the displacement and rotation required for placing the ensuing WHB domain and its linked NEDD8 at the center of the ubiquitylation complex.

Extended Data Figure 6 |. Geometry between phosphodegron and acceptor in structure, substrates, and ubiquitylation.

a, Cryo EM density highlighting the relative placement of substrate degron and UBE2D~UB active site. The ~22Å distance between UBE2D~UB active site and the phosphodegron of β-TRCP-bound substrate requires at least 6 intervening residues in a substrate. **b**, Alignments for several reported β-TRCP substrates[32], highlighting the degron sequence (yellow) and nearby lysines (red). Also shown are sequences of peptide substrates with a single acceptor Lys that were used in kinetics analyses. The peptide sequences were derived from IκBα, and from β-catenin with varying spacers between phosphodegron and acceptor Lys: WT β-catenin peptide, "medium" β-catenin peptide with lysine corresponding to IκBα, and "short" β-catenin peptide with a lysine 5 residues upstream of the N-terminal phosphoSer in

the degron, which would be too short to bridge the structurally-observed distance between the phosphodegron binding site on β-TRCP and UBE2D catalytic Cys in the ubiquitylation active site. **c**, Representative autoradiogram (n = 2) of SDS-PAGE gel showing products from indicated time points of ubiquitylation reactions under multi-turnover conditions with either neddylated or unneddylated $CRL1^{\beta\text{-}TRCP}$ and radiolabeled short β-catenin peptide substrate. The amount of short β-catenin peptide modified by neddylated $CRL1^{\beta\text{-}TRCP}$ and UBE2D is too low in the single-encounter ubiquitylation reaction to allow quantification of kinetic parameters, yet, product formation is apparent under multi-turnover conditions and shows that most products are heavily ubiquitylated. **d**, Plots fitting consumption of unmodified short β-catenin peptide substrate (S0) compared to formation of polyubiquitin chains with 5 or more UBs (S5+) from reactions as in panel **c**. The symbols show the data from independent experiments (n = 2 technical replicates).

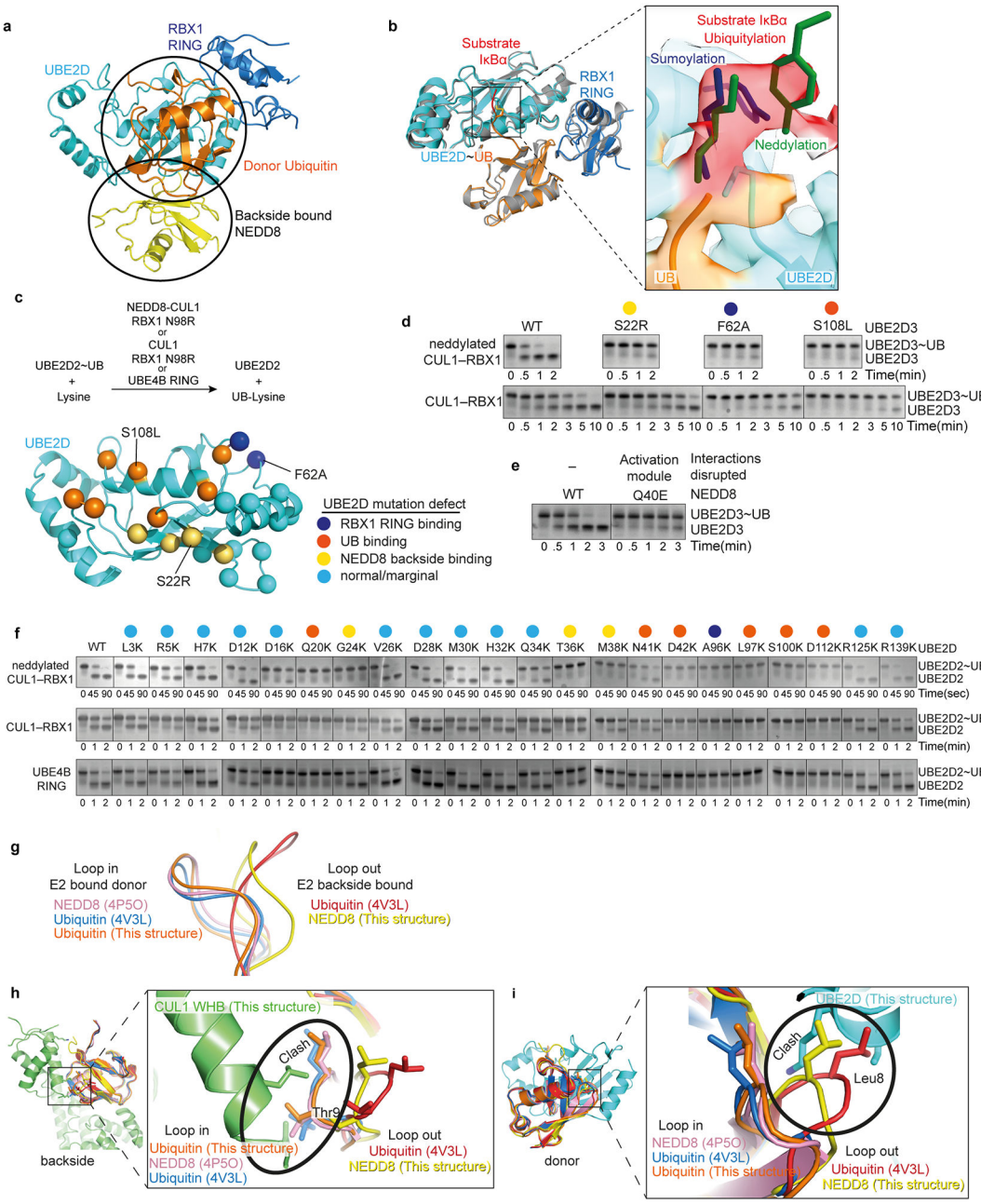

Extended Data Figure 7 |. Interactions shaping the catalytic architecture of neddylated CRL1$^{\beta\text{-TRCP}}$-UBE2D~UB-IκBα substrate intermediate.

a, NEDD8 and the catalytic module from the structure representing the neddylated CRL1$^{\beta\text{-TRCP}}$-UBE2D~UB-IκBα intermediate, highlighting distinctive interactions between NEDD8 (yellow) and donor UB (orange) with UBE2D. **b**, Catalytic module from the neddylated CRL1$^{\beta\text{-TRCP}}$-UBE2D~UB-IκBα intermediate, highlighting the covalently-linked proxy for the IκBα substrate's acceptor in the active site relative to a superimposed representative prior crystal structure of an isolated RING-UBE2D~UB complex (grey, PDB: 4AP4)[28,29]. In the inset, the density for the covalently-linked proxy for IκBα substrate's acceptor is shown in red the active site. The chemical trap superimposes with consensus

acceptors visualized in active sites of sumoylation and neddylation intermediates, where aromatic side-chains guide the lysine targets (blue and green, respectively)[39,73]. However, UBE2D's myriad substrates neither conform to a specific motif, nor do they or UBE2D display specific side-chains guiding lysine acceptors into the catalytic center. Instead, in the neddylated CRL1$^{\beta\text{-TRCP}}$-UBE2D~UB-substrate complex, density from backbone atoms preceding the chemical proxy for the acceptor Lys corresponds to the aromatic guides in sumoylation and neddylation intermediates. **c**, Overview of assays for activation of intrinsic reactivity of UBE2D~UB intermediate. Top, schematic of pulse-chase assay for testing effects of UBE2D mutations on activation, monitoring UBE2D~UB discharge to free lysine activated by neddylated CUL-RBX1 compared to unneddylated or RING-like UBE4B controls. Bottom, sites of mutations shown as spheres on structure of UBE2D from cryo EM structure of neddylated CRL1$^{\beta\text{-TRCP}}$-UBE2D~UB-substrate complex. Sphere colors reflect both the locations and the effects on UBE2D~UB discharge to free lysine. Sites of mutations with marginal or no effect are shown in cyan, whereas those with major effects are colored. Mutations causing major defects map to RBX1 RING-binding site (blue), the interaction surface with the donor UB (orange), and the interaction surface with NEDD8 (yellow). **d**, Representative Coommassie-stained SDS-PAGE gels (of two independent experiments) shown for reactions monitoring substrate-independent discharge of UBE2D~UB to free lysine, in presence of CUL1-RBX1 (N98R) that was either neddylated or unneddylated (K720R), with either WT or indicated UBE2D3 mutants at binding sites for backside-bound NEDD8 (S22R), the RBX1 RING (F62A), and the covalently-linked donor UB in the closed conformation (S108L). **e**, Same as in **d** except testing effect of NEDD8 Q40E, which would disrupt the activation module. **f**, Reactions performed as in **d**, except with indicated variants of UBE2D2, in reactions with CUL1-RBX1 (N98R) that was either neddylated or unneddylated (K720R), or with the optimized RING-like U-box domain from UBE4B as a reference[58]. For mutations reporting on the catalytic conformation (G24K, T36K, M38K, A96K and D112K), representative gels are shown for two experiments. All other experiments were performed once. **g**, Comparison of β1/β2 -loop conformations after superimposing the indicated structures of NEDD8 and UB. The comparison suggests that while NEDD8 and UB can adopt both "loop in" and "loop out" conformations, donors linked to E2 active sites in RING activated complexes adopt the "loop in" conformation, and those bound to UBE2D backside adopt "loop out" conformations. **h**, Only a "loop out" conformation is compatible with the neddylated CRL activation module structure, because "loop in" conformation from the structures shown in **g** would prevent noncovalent interactions with CUL1 WHB domain (green). **i**, Only a "loop out" conformation is compatible for the CUL1-linked NEDD8 to bind the catalytic module, because "loop in" conformations in the structures shown in **g** would prevent noncovalent interactions with the UBE2D backside (cyan).

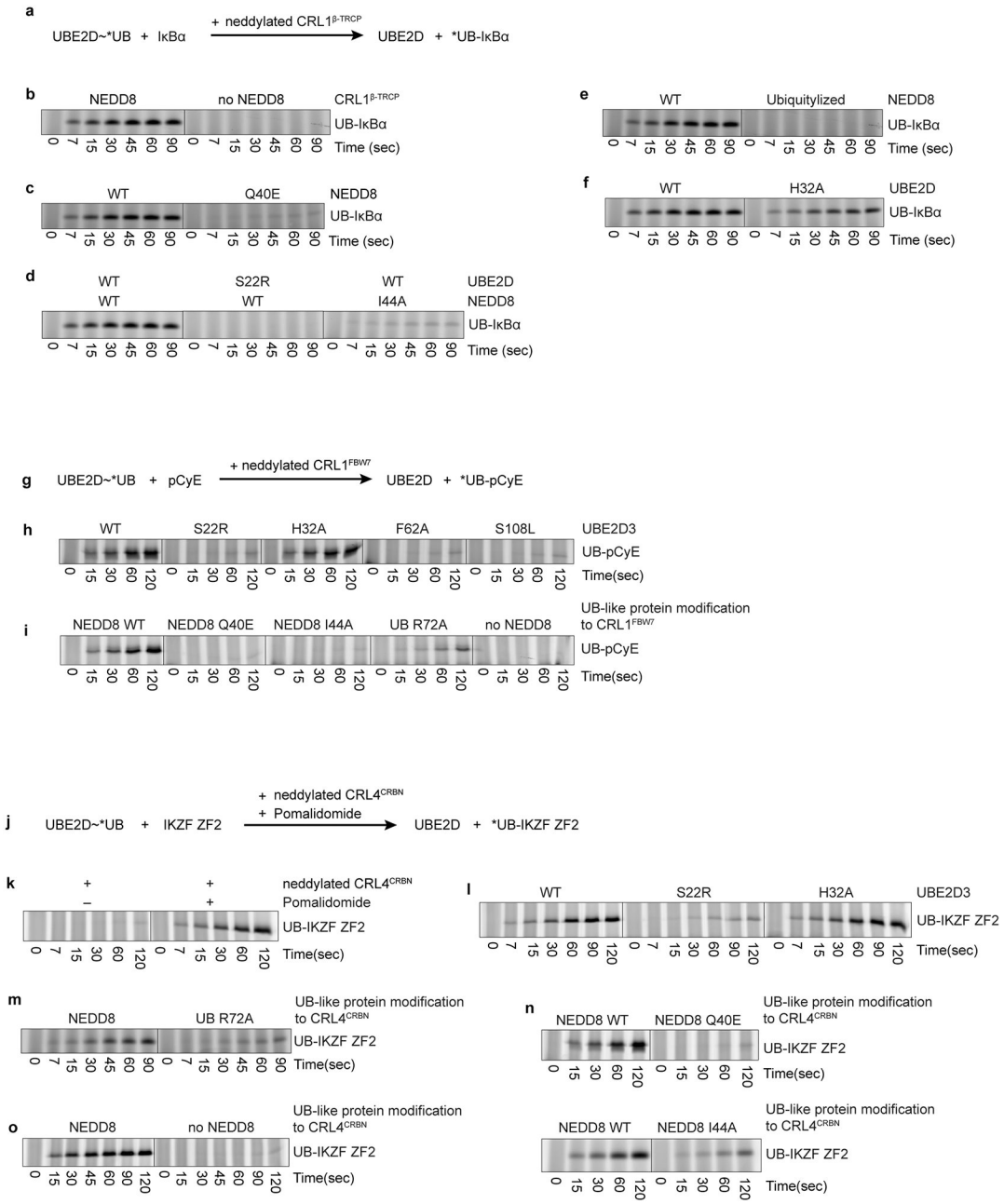

Extended Data Figure 8 |. Qualitative validation of mechanistic principles underlying substrate priming by neddylated CRLs and UBE2D.

Gel panels in this figure are representative from two independent experiments; n=2 technical replicates.

a, Schematic of a qualitative substrate priming assay for testing effects of mutations in neddylated CRL1$^{\beta\text{-TRCP}}$ or UBE2D on substrate priming, monitoring fluorescent UB transfer from UBE2D3 to the phosphorylated IκBα substrate. **b**, Scan of SDS-PAGE detecting fluorescent UB transferred to IκBα-derived substrate in qualitative assay for NEDD8 activation of substrate priming. **c**, as in **b**, showing effect on substrate priming of disrupting the activation module with the NEDD8 Q40E mutation. **d**, as in **b**, showing the

effect on substrate priming of disrupting interactions between the activation and catalytic modules with NEDD8 I44A or UBE2D S22R mutation. **e**, as in **b**, showing the effect on substrate priming of disrupting interactions between the activation and substrate scaffolding modules, though CUL1 modification by a "Ubiquitylized" NEDD8 mutant with six residues swapped for UB counterparts (L2Q K4F E14T D16E G63K G64E). **f**, as in **b**, showing the effect of UBE2D H32A mutation at the interface between the catalytic and substrate scaffolding modules. **g**, Scheme of pulse-chase assay for testing effects of mutations in neddylated $CRL1^{FBW7}$ or UBE2D on substrate priming. Assay monitors transfer of fluorescent UB from UBE2D to peptide substrate derived from phosphorylated Cyclin E (pCyE). **h**, Fluorescent scan detecting UB transferred to the pCyE substrate by neddylated $CRL1^{FBW7}$ and the indicated mutants of UBE2D. **i**, Fluorescent scan detecting UB transferred to the pCyE substrate by UBE2D and indicated variants of neddylated (or ubiquitylated) $CRL1^{FBW7}$. Experiment with unneddylated $CRL1^{FBW7}$ use the K720R variant of CUL1 to prevent artifactual ubiquitylation.

j, Scheme of pulse-chase assay for testing effects of mutations in neddylated $CRL4^{CRBN}$ or UBE2D on substrate priming, monitoring fluorescent UB transfer from UBE2D to the IKZF1/3 ZF2 substrate in the presence of the immunomodulatory drug pomalidomide. **k**, Fluorescent scan of assay validation, showing pomalidomide-dependence. **l**, Fluorescent scan detecting UB transferred to the IKZF substrate by $CRL4^{CRBN}$, pomalidomide and the indicated variants of UBE2D. **m-o**, Fluorescent scan detecting UB transferred to the IKZF substrate by UBE2D and the indicated variants of neddylated (or ubiquitylated) $CRL4^{CRBN}$ with pomalidomide. Experiments with unneddylated $CRL4^{CRBN}$ use the K705R variant of CUL4A to prevent artifactual ubiquitylation.

Extended Data Table 1 |

Estimates of K_m and k_{obs} for Substrate Ubiquitylation.

Substrate	E2	$CRL1^{\beta\text{-}TRCP}$	$K_m(10^{-9}M)$	k_{obs}^{S0-S1} (sec^{-1})	k_{obs}^{S1-S2} (sec^{-1})	k_{obs}^{S0-S1}/K_m ($M^{-1}sec^{-1}$)	Fold change
IκBα	WT UBE2D	NEDD8-CUL1–RBX1	408 ± 57	12.9 ± 1.7	0.24 ± 0.04	3.2×10^7	-
IκBα	WT UBE2D	CUL1–RBX1	4014 ±956	0.05 ± 0.002	-	1.2×10^4	2667
WT β-cat	WT UBE2D	NEDD8-CUL1–RBX1	214 ±30	4.8 ±0.46	0.19 ±0.02	2.2×10^7	-
WT β-cat	WT UBE2D	CUL1–RBX1	4638±138	0.05 ± 0.005	-	1.1×10^4	2000
medium β-cat	WT UBE2D	NEDD8-CUL1–RBX1	372 ± 48	11 ± 1.00	0.24 ± 0.04	3.0×10^7	-
medium β-cat	WT UBE2D	CUL1–RBX1	4875 ±1328	0.08 ± 0.005	-	1.6×10^4	1875
short β-cat	WT UBE2D	CUL1–RBX1	5207±1051	0.02 ± 0.0004	-	3.8×10^3	
medium β-cat	WT UBE2D	NEDD8 I44A-CUL1–RBX1	1087 ±69	3.60 ±0.27	0.17 ±0.03	3.3×10^6	9.1
medium β-cat	WT UBE2D	UB-CUL1–RBX1	2056 ±170	1.0 ±0.03	0.15 ±0.01	4.9×10^5	61.2

Substrate	E2	CRL1$^{\beta\text{-TRCP}}$	K_m(10^{-9}M)	k_{obs}^{S0-S1} (sec^{-1})	k_{obs}^{S1-S2} (sec^{-1})	k_{obs}^{S0-S1}/K_m ($M^{-1}sec^{-1}$)	Fold change
medium β-cat	WT UBE2D	NEDD8 Q40E-CUL1–RBX1	1941 ±226	1.77 ± 0.13	0.07 ±0.01	9.1×10^5	33.0
medium β-cat	WT UBE2D	UBylized NEDD8-CUL1–RBX1	1651±137	2.20 ±0.15	0.17 ±0.04	1.3×10^6	23.1
medium β-cat	S22R UBE2D	NEDD8-CUL1–RBX1	913 ±135	1.89 ±0.14	0.17 ±0.03	2.1×10^6	14.2
medium β-cat	S22R UBE2D	NEDD8 I44A-CUL1–RBX1	5190 ±604	0.13 ±0.01	-	2.5×10^4	1200
medium β-cat	S22R UBE2D	UB-CUL1–RBX1	6492 ± 872	0.08 ± 0.005	-	1.2×10^4	2500
medium β-cat	S22R UBE2D	CUL1–RBX1	4007 ± 754	0.013 ±0.002	-	3.3×10^3	9091
medium β-cat	S22R UBE2D	NEDD8 Q40E-CUL1–RBX1	3581 ± 367	0.17 ±0.005	-	4.7×10^4	638.3
medium β-cat	S22R UBE2D	UBylized NEDD8-CUL1–RBX1	6105 ±1030	0.12 ±0.007	-	2.0×10^4	1500
medium β-cat	H32A UBE2D	NEDD8-CUL1–RBX1	347 ± 53	8.15 ± 1.04	0.73 ± 0.09	2.3×10^7	1.3
medium β-cat	H32A UBE2D	NEDD8 I44A-CUL1–RBX1	3431 ± 332	0.58 ± 0.04	0.12 ±0.02	1.7×10^5	176.5
medium β-cat	H32A UBE2D	UB-CUL1–RBX1	2999 ± 301	0.34 ±0.01	0.10 ±0.02	1.1×10^5	272.7
medium β-cat	H32A UBE2D	CUL1–RBX1	3305 ±1119	0.06 ± 0.003	-	1.8×10^4	1666.7
medium β-cat	H32A UBE2D	NEDD8 Q40E-CUL1–RBX1	2923 ± 459	0.81 ±0.06	-	2.8×10^5	107.1
medium β-cat	H32A UBE2D	UBylized NEDD8-CUL1–RBX1	4303 ±310	0.28 ± 0.02	-	6.5×10^4	461.5
UB-β-cat	WT UBE2D	NEDD8-CUL1–RBX1	148 ± 15	-	0.48 ± 0.02		
UB-β-cat	WT UBE2D	CUL1–RBX1	1503 ±439	-	0.005 ± 0.0004		

S0 refers to unmodified substrate, S1 to substrate modified by a single UB, and S2 to substrate modified with two UBs. S0-S1 refers to the transition from unmodified to UB-substrate, and S1-S2 to the transition from UB-substrate to UB-UB-substrate. Values for K_m are the best fit values derived from nonlinear regression in Prism, and value for k_{obs} are the best fit values derived from nonlinear regression in Mathematica. The measure of error is the standard error as determined by Prism and Mathematica, respectively, from experiments and curve fits such as those shown in Extended Data Figure 1 (n=2).

Extended Data Table 2 |

Cryo-EM data collection, refinement, and validation statistics.

IκBα–UB~UBE2D crosslink	UBE2D2	UBE2D3	UBE2D3	UBE2D2	UBE2D2	none	none
(C21I C107A Cl 1 ID)	2×2way XL	3way XL	3way XL	3way XL	3way XL		
Substrate Receptor	β-TRCP2	β-TRCP1	β-TRCP1	β-TRCP1	β-TRCP1	β-TRCP1	β-TRCP1
		175-C	175-C	175-C	175-C	175-C	175-C

RBX1	WT	WT	N98R	N98R	N98R	WT	WT
NEDD8	yes	yes	yes	yes	yes	no	yes
SKP1	WT	ΔΔ	ΔΔ	ΔΔ	ΔΔ	WT	WT
	EMDB-10578	EMDB-10579	EMDB-10580	EMDB-10581	EMDB-10585 PDB 6TTU	EMDB-10582	EMDB-10583
Data collection and processing							
Microscope	Krios	Arctica	Arctica	Arctica	Krios	Glacios	Glacios
Magnification	105,000	92,000	73,000	73,000	130,000	36,000	22,000
Voltage (kV)	300	200	200	200	300	200	200
Electron exposure (e−/Å^2)	56	61.3	60.8	70	70.2	60	59
Defocus range (μm)	−1.2 ~ −3.6	−1.5 ~ −3.5	−1.5 ~ −3.5	−1.5 ~ −3.5	−1.2 ~ −3.3	−1.2 ~ −3.3	−1.2 ~ −3.3
Pixel size (Å)	1.34	1.612	1.997	1.997	1.06	1.181	1.885
Symmetiy imposed	C2	Cl	Cl	Cl	Cl	Cl	Cl
Initial particle images (no.)	2,575,161	464,344	601,121	459,011	1,661,870	2,051,804	1,666,293
Final particle images (no.)	33,738	47,246	107,311	40,835	106,257	262,116	349,803
Map resolution (Å)	9.3	8.6	9.4	8.4	3.72	4.64	6.7
FSC threshold	(0.143)	(0.143)	(0.143)	(0.143)	(0.143)	(0.143)	(0.143)
Map resolution range (Å)	-	-	-	-	3.46~6.0	-	-
Refinement							
Initial model used					1LDJ 1P22		
(PDB code)					4P5O 4V3L		
Model resolution (Å)					3.7		
FSC threshold					(0.143)		
Map sharpening *B* factor (Å^2)	−578.9	−1159	−1272	−983.5	−94.2	−199	−338
Model composition							
Non-hydrogen atoms					13034		
Protein residues					1616		
Ligands					3(ZN)		
B factors (Å^2)							
Protein					91		
Ligand					224		

R.m.s. deviations	
Bond lengths (Å)	0.011
Bond angles (°)	1.043
Validation	
MolProbity score	2.37
Clashscore	16.31
Poor rotamers (%)	0.21
Ramachandran plot	
Favored (%)	85.12
Allowed (%)	14.88
Disallowed (%)	0

Supplementary Material

Refer to Web version on PubMed Central for supplementary material.

Acknowledgements

We are grateful to D. Scott, J. Kellermann, J. Liwocha, S. Kostrhon, D. Horn-Ghetko, J.W. Harper, R.V. Farese Jr., H. Stark, D. Haselbach, S. Raunser, T. Raisch, S. Scheres, S. Uebel, S. Pettera for assistance, reagents, and helpful discussions. We thank M. Strauss, D. Bollschweiler, T. Schäfer and the cryo EM facility at Max Planck Institute of Biochemistry. This study was supported by the Max Planck Gesellschaft and by grants of the European Commission (ERC Advanced Investigator Grant Nedd8Activate), the Deutsche Forschungsgemeinschaft (DFG Gottfried Wilhelm Leibniz Prize to BAS). SH and GK were supported by a grant of the National Institutes of Health (R15GM117555-02).

References

1. Lydeard JR, Schulman BA & Harper JW Building and remodelling Cullin-RING E3 ubiquitin ligases. EMBO reports 14, 1050–1061, doi:10.1038/embor.2013.173 (2013). [PubMed: 24232186]
2. Read MA et al. Nedd8 modification of cul-1 activates SCF(beta(TrCP))-dependent ubiquitination of IkappaBalpha. Molecular and cellular biology 20, 2326–2333 (2000). [PubMed: 10713156]
3. Duda DM et al. Structural insights into NEDD8 activation of cullin-RING ligases: conformational control of conjugation. Cell 134, 995–1006 (2008). [PubMed: 18805092]
4. Saha A & Deshaies RJ Multimodal activation of the ubiquitin ligase SCF by Nedd8 conjugation. Molecular cell 32, 21–31 (2008). [PubMed: 18851830]
5. Yamoah K et al. Autoinhibitory regulation of SCF-mediated ubiquitination by human cullin 1's C-terminal tail. Proceedings of the National Academy of Sciences of the United States of America 105, 12230–12235 (2008). [PubMed: 18723677]
6. Soucy TA et al. An inhibitor of NEDD8-activating enzyme as a new approach to treat cancer. Nature 458, 732–736, doi:nature07884 [pii] 10.1038/nature07884 (2009). [PubMed: 19360080]
7. Zheng N et al. Structure of the Cul1-Rbx1-Skp1-F boxSkp2 SCF ubiquitin ligase complex. Nature 416, 703–709 (2002). [PubMed: 11961546]
8. Jin J et al. Systematic analysis and nomenclature of mammalian F-box proteins. Genes & development 18, 2573–2580, doi:10.1101/gad.1255304 (2004). [PubMed: 15520277]

9. Willems AR, Schwab M & Tyers M A hitchhiker's guide to the cullin ubiquitin ligases: SCF and its kin. Biochimica et biophysica acta 1695, 133–170 (2004). [PubMed: 15571813]
10. Angers S et al. Molecular architecture and assembly of the DDB1-CUL4A ubiquitin ligase machinery. Nature 443, 590–593 (2006). [PubMed: 16964240]
11. Jin J, Arias EE, Chen J, Harper JW & Walter JC A family of diverse Cul4-Ddb1-interacting proteins includes Cdt2, which is required for S phase destruction of the replication factor Cdt1. Molecular cell 23, 709–721 (2006). [PubMed: 16949367]
12. Yu C et al. Gln40 deamidation blocks structural reconfiguration and activation of SCF ubiquitin ligase complex by Nedd8. Nature communications 6, 10053, doi:10.1038/ncomms10053 (2015).
13. Pierce NW et al. Cand1 promotes assembly of new SCF complexes through dynamic exchange of F box proteins. Cell 153, 206–215, doi:10.1016/j.cell.2013.02.024 (2013). [PubMed: 23453757]
14. Stanley DJ et al. Inhibition of a NEDD8 Cascade Restores Restriction of HIV by APOBEC3G. PLoS Pathog 8, e1003085, doi:10.1371/journal.ppat.1003085 (2012). [PubMed: 23300442]
15. Yaron A et al. Identification of the receptor component of the IkappaBalpha-ubiquitin ligase. Nature 396, 590–594, doi:10.1038/25159 (1998). [PubMed: 9859996]
16. Winston JT et al. The SCFbeta-TRCP-ubiquitin ligase complex associates specifically with phosphorylated destruction motifs in IkappaBalpha and beta-catenin and stimulates IkappaBalpha ubiquitination in vitro. Genes & development 13, 270–283 (1999). [PubMed: 9990852]
17. Spencer E, Jiang J & Chen ZJ Signal-induced ubiquitination of IkappaBalpha by the F-box protein Slimb/beta-TrCP. Genes & development 13, 284–294, doi:10.1101/gad.13.3.284 (1999). [PubMed: 9990853]
18. Hart M et al. The F-box protein beta-TrCP associates with phosphorylated beta-catenin and regulates its activity in the cell. Curr Biol 9, 207–210, doi:10.1016/s0960-9822(99)80091-8 (1999). [PubMed: 10074433]
19. Latres E, Chiaur DS & Pagano M The human F box protein beta-Trcp associates with the Cul1/Skp1 complex and regulates the stability of beta-catenin. Oncogene 18, 849–854, doi:10.1038/sj.onc.1202653 (1999). [PubMed: 10023660]
20. Wu G et al. Structure of a beta-TrCP1-Skp1-beta-catenin complex: destruction motif binding and lysine specificity of the SCF(beta-TrCP1) ubiquitin ligase. Molecular cell 11, 1445–1456 (2003). [PubMed: 12820959]
21. Wu K, Kovacev J & Pan ZQ Priming and extending: a UbcH5/Cdc34 E2 handoff mechanism for polyubiquitination on a SCF substrate. Molecular cell 37, 784–796, doi:S1097–2765(10)00208-X [pii] 10.1016/j.molcel.2010.02.025 (2010). [PubMed: 20347421]
22. Frescas D & Pagano M Deregulated proteolysis by the F-box proteins SKP2 and beta-TrCP: tipping the scales of cancer. Nat Rev Cancer 8, 438–449, doi:10.1038/nrc2396 (2008). [PubMed: 18500245]
23. Margottin F et al. A novel human WD protein, h-beta TrCp, that interacts with HIV-1 Vpu connects CD4 to the ER degradation pathway through an F-box motif. Molecular cell 1, 565–574 (1998). [PubMed: 9660940]
24. Cui J et al. Glutamine deamidation and dysfunction of ubiquitin/NEDD8 induced by a bacterial effector family. Science (New York, N.Y 329, 1215–1218, doi:10.1126/science.1193844 (2010).
25. Jubelin G et al. Pathogenic bacteria target NEDD8-conjugated cullins to hijack host-cell signaling pathways. PLoS Pathog 6, doi:10.1371/journal.ppat.1001128 (2010).
26. Morikawa H et al. The bacterial effector Cif interferes with SCF ubiquitin ligase function by inhibiting deneddylation of Cullin1. Biochemical and biophysical research communications 401, 268–274, doi:10.1016/j.bbrc.2010.09.048 (2010). [PubMed: 20850415]
27. Tang X et al. Suprafacial orientation of the SCFCdc4 dimer accommodates multiple geometries for substrate ubiquitination. Cell 129, 1165–1176 (2007). [PubMed: 17574027]
28. Dou H, Buetow L, Sibbet GJ, Cameron K & Huang DT BIRC7-E2 ubiquitin conjugate structure reveals the mechanism of ubiquitin transfer by a RING dimer. Nature structural & molecular biology 19, 876–883, doi:10.1038/nsmb.2379 (2012).
29. Plechanovova A, Jaffray EG, Tatham MH, Naismith JH & Hay RT Structure of a RING E3 ligase and ubiquitin-loaded E2 primed for catalysis. Nature 489, 115–120, doi:10.1038/nature11376 (2012). [PubMed: 22842904]

30. Pruneda JN et al. Structure of an E3:E2 approximately Ub Complex Reveals an Allosteric Mechanism Shared among RING/U-box Ligases. Molecular cell 47, 933–942, doi:10.1016/j.molcel.2012.07.001 (2012). [PubMed: 22885007]

31. Brzovic PS & Klevit RE Ubiquitin transfer from the E2 perspective: why is UbcH5 so promiscuous? Cell cycle (Georgetown, Tex 5, 2867–2873, doi:10.4161/cc.5.24.3592 (2006).

32. Low TY et al. A systems-wide screen identifies substrates of the SCFbetaTrCP ubiquitin ligase. Science signaling 7, rs8, doi:10.1126/scisignal.2005882 (2014). [PubMed: 25515538]

33. Lumb KJ & Kim PS A buried polar interaction imparts structural uniqueness in a designed heterodimeric coiled coil. Biochemistry 34, 8642–8648, doi:10.1021/bi00027a013 (1995). [PubMed: 7612604]

34. Kawakami T et al. NEDD8 recruits E2-ubiquitin to SCF E3 ligase. The EMBO journal 20, 4003–4012 (2001). [PubMed: 11483504]

35. Ozkan E, Yu H & Deisenhofer J Mechanistic insight into the allosteric activation of a ubiquitin-conjugating enzyme by RING-type ubiquitin ligases. Proceedings of the National Academy of Sciences of the United States of America 102, 18890–18895 (2005). [PubMed: 16365295]

36. Brzovic PS, Lissounov A, Christensen DE, Hoyt DW & Klevit RE A UbcH5/ubiquitin noncovalent complex is required for processive BRCA1-directed ubiquitination. Molecular cell 21, 873–880 (2006). [PubMed: 16543155]

37. Sakata E et al. Direct interactions between NEDD8 and ubiquitin E2 conjugating enzymes upregulate cullin-based E3 ligase activity. Nature structural & molecular biology 14, 167–168 (2007).

38. Buetow L et al. Activation of a primed RING E3-E2-ubiquitin complex by non-covalent ubiquitin. Molecular cell 58, 297–310, doi:10.1016/j.molcel.2015.02.017 (2015). [PubMed: 25801170]

39. Scott DC et al. Structure of a RING E3 Trapped in Action Reveals Ligation Mechanism for the Ubiquitin-like Protein NEDD8. Cell 157, 1671–1684, doi:10.1016/j.cell.2014.04.037 (2014). [PubMed: 24949976]

40. Hospenthal MK, Freund SM & Komander D Assembly, analysis and architecture of atypical ubiquitin chains. Nature structural & molecular biology 20, 555–565, doi:10.1038/nsmb.2547 (2013).

41. Scott DC et al. Two Distinct Types of E3 Ligases Work in Unison to Regulate Substrate Ubiquitylation. Cell 166, 1198–1214 e1124, doi:10.1016/j.cell.2016.07.027 (2016). [PubMed: 27565346]

42. Huttenhain R et al. ARIH2 Is a Vif-Dependent Regulator of CUL5-Mediated APOBEC3G Degradation in HIV Infection. Cell Host Microbe 26, 86–99 e87, doi:10.1016/j.chom.2019.05.008 (2019). [PubMed: 31253590]

43. Hill S et al. Robust cullin-RING ligase function is established by a multiplicity of poly-ubiquitylation pathways. Elife 8, doi:10.7554/eLife.51163 (2019).

44. den Besten W, Verma R, Kleiger G, Oania RS & Deshaies RJ NEDD8 links cullin-RING ubiquitin ligase function to the p97 pathway. Nature structural & molecular biology 19, 511–516, S511, doi:10.1038/nsmb.2269 (2012).

45. Schapira M, Calabrese MF, Bullock AN & Crews CM Targeted protein degradation: expanding the toolbox. Nat Rev Drug Discov 18, 949–963, doi:10.1038/s41573-019-0047-y (2019). [PubMed: 31666732]

46. Goldenberg SJ et al. Structure of the Cand1-Cul1-Roc1 complex reveals regulatory mechanisms for the assembly of the multisubunit cullin-dependent ubiquitin ligases. Cell 119, 517–528 (2004). [PubMed: 15537541]

47. Mosadeghi R et al. Structural and kinetic analysis of the COP9-Signalosome activation and the cullin-RING ubiquitin ligase deneddylation cycle. Elife 5, doi:10.7554/eLife.12102 (2016).

48. Cavadini S et al. Cullin-RING ubiquitin E3 ligase regulation by the COP9 signalosome. Nature 531, 598–603, doi:10.1038/nature17416 (2016). [PubMed: 27029275]

49. Liu X et al. Cand1-Mediated Adaptive Exchange Mechanism Enables Variation in F-Box Protein Expression. Molecular cell 69, 773–786 e776, doi:10.1016/j.molcel.2018.01.038 (2018). [PubMed: 29499133]

50. Kamadurai HB et al. Insights into ubiquitin transfer cascades from a structure of a UbcH5B approximately ubiquitin-HECT(NEDD4L) complex. Molecular cell 36, 1095–1102, doi:S1097–2765(09)00824–7 [pii] 10.1016/j.molcel.2009.11.010 (2009). [PubMed: 20064473]
51. Brown NG et al. Mechanism of polyubiquitination by human anaphase-promoting complex: RING repurposing for ubiquitin chain assembly. Molecular cell 56, 246–260, doi:10.1016/j.molcel.2014.09.009 (2014). [PubMed: 25306923]
52. Weissmann F et al. biGBac enables rapid gene assembly for the expression of large multisubunit protein complexes. Proceedings of the National Academy of Sciences of the United States of America 113, E2564–2569, doi:10.1073/pnas.1604935113 (2016). [PubMed: 27114506]
53. Hao B, Oehlmann S, Sowa ME, Harper JW & Pavletich NP Structure of a Fbw7-Skp1-cyclin E complex: multisite-phosphorylated substrate recognition by SCF ubiquitin ligases. Molecular cell 26, 131–143 (2007). [PubMed: 17434132]
54. Schulman BA et al. Insights into SCF ubiquitin ligases from the structure of the Skp1-Skp2 complex. Nature 408, 381–386 (2000). [PubMed: 11099048]
55. Walden H et al. The structure of the APPBP1-UBA3-NEDD8-ATP complex reveals the basis for selective ubiquitin-like protein activation by an E1. Molecular cell 12, 1427–1437 (2003). [PubMed: 14690597]
56. Whitby FG, Xia G, Pickart CM & Hill CP Crystal structure of the human ubiquitin-like protein NEDD8 and interactions with ubiquitin pathway enzymes. The Journal of biological chemistry 273, 34983–34991 (1998). [PubMed: 9857030]
57. Koduri V et al. Peptidic degron for IMiD-induced degradation of heterologous proteins. Proceedings of the National Academy of Sciences of the United States of America 116, 2539–2544, doi:10.1073/pnas.1818109116 (2019). [PubMed: 30683719]
58. Starita LM et al. Activity-enhancing mutations in an E3 ubiquitin ligase identified by high-throughput mutagenesis. Proceedings of the National Academy of Sciences of the United States of America 110, E1263–1272, doi:10.1073/pnas.1303309110 (2013). [PubMed: 23509263]
59. Pierce NW, Kleiger G, Shan SO & Deshaies RJ Detection of sequential polyubiquitylation on a millisecond timescale. Nature 462, 615–619, doi:nature08595 [pii] 10.1038/nature08595 (2009). [PubMed: 19956254]
60. Sievers QL et al. Defining the human C2H2 zinc finger degrome targeted by thalidomide analogs through CRBN. Science (New York, N.Y 362, doi:10.1126/science.aat0572 (2018).
61. Lu G et al. UBE2G1 governs the destruction of cereblon neomorphic substrates. Elife 7, doi:10.7554/eLife.40958 (2018).
62. Gibson DG et al. Enzymatic assembly of DNA molecules up to several hundred kilobases. Nat Methods 6, 343–345, doi:10.1038/nmeth.1318 (2009). [PubMed: 19363495]
63. Streich FC Jr. & Lima CD Capturing a substrate in an activated RING E3/E2-SUMO complex. Nature 536, 304–308, doi:10.1038/nature19071 (2016). [PubMed: 27509863]
64. Kastner B et al. GraFix: sample preparation for single-particle electron cryomicroscopy. Nat Methods 5, 53–55, doi:10.1038/nmeth1139 (2008). [PubMed: 18157137]
65. Palovcak E et al. A simple and robust procedure for preparing graphene-oxide cryo-EM grids. J Struct Biol 204, 80–84, doi:10.1016/j.jsb.2018.07.007 (2018). [PubMed: 30017701]
66. Zivanov J et al. New tools for automated high-resolution cryo-EM structure determination in RELION-3. Elife 7, doi:10.7554/eLife.42166 (2018).
67. Rohou A & Grigorieff N CTFFIND4: Fast and accurate defocus estimation from electron micrographs. J Struct Biol 192, 216–221, doi:10.1016/j.jsb.2015.08.008 (2015). [PubMed: 26278980]
68. Hohn M et al. SPARX, a new environment for Cryo-EM image processing. J Struct Biol 157, 47–55, doi:10.1016/j.jsb.2006.07.003 (2007). [PubMed: 16931051]
69. Pettersen EF et al. UCSF Chimera--a visualization system for exploratory research and analysis. J Comput Chem 25, 1605–1612, doi:10.1002/jcc.20084 (2004). [PubMed: 15264254]
70. Emsley P, Lohkamp B, Scott WG & Cowtan K Features and development of Coot. Acta crystallographica 66, 486–501, doi:S0907444910007493 [pii] 10.1107/S0907444910007493 (2010). [PubMed: 20383002]

71. Afonine PV et al. New tools for the analysis and validation of cryo-EM maps and atomic models. Acta Crystallogr D Struct Biol 74, 814–840, doi:10.1107/S2059798318009324 (2018). [PubMed: 30198894]

72. Duda DM et al. Structure of a glomulin-RBX1-CUL1 complex: inhibition of a RING E3 ligase through masking of its E2-binding surface. Molecular cell 47, 371–382, doi:10.1016/j.molcel.2012.05.044 (2012). [PubMed: 22748924]

73. Yunus AA & Lima CD Lysine activation and functional analysis of E2-mediated conjugation in the SUMO pathway. Nature structural & molecular biology 13, 491–499 (2006).

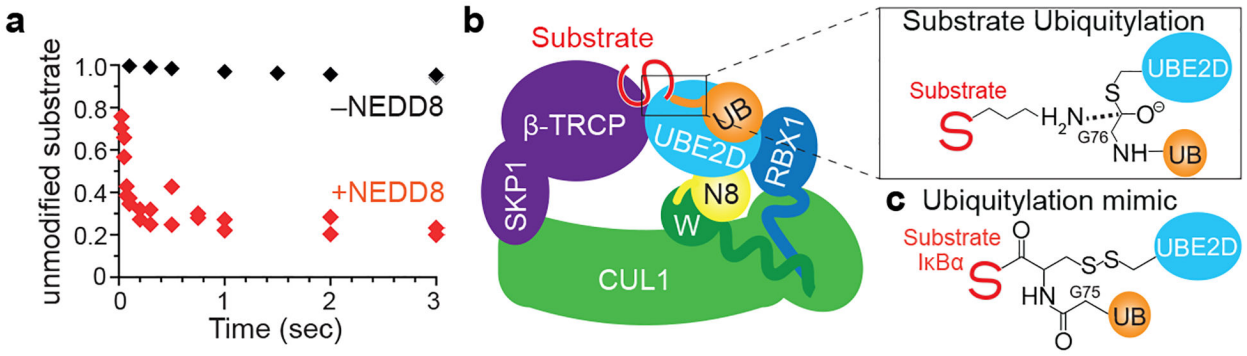

Figure 1 |. Role of NEDD8 and strategy to visualize dynamic ubiquitin transfer from E2 UBE2D to substrate by neddylated CRL1$^{β\text{-}TRCP}$

a, Effect of CUL1 neddylation on CRL1$^{β\text{-}TRCP}$-catalyzed UB transfer from E2 UBE2D to a radiolabeled β-catenin-derived peptide substrate. Plots show substrate remaining during pre-steady-state rapid quench-flow ubiquitylation reactions with saturating UBE2D3 and either unneddylated or neddylated CRL1$^{β\text{-}TRCP}$. The symbols show the data from independent experiments (n = 2 technical replicates). **b**, Cartoon representing substrate priming by neddylated CRL1$^{β\text{-}TRCP}$ and UBE2D~UB. Inset shows transition state during ubiquitylation. **c**, Chemical mimic of the ubiquitylation intermediate, where surrogates for the active site of UBE2D, the C-terminus of UB, and the UB acceptor site on the IκBα-derived substrate peptide are simultaneously linked.

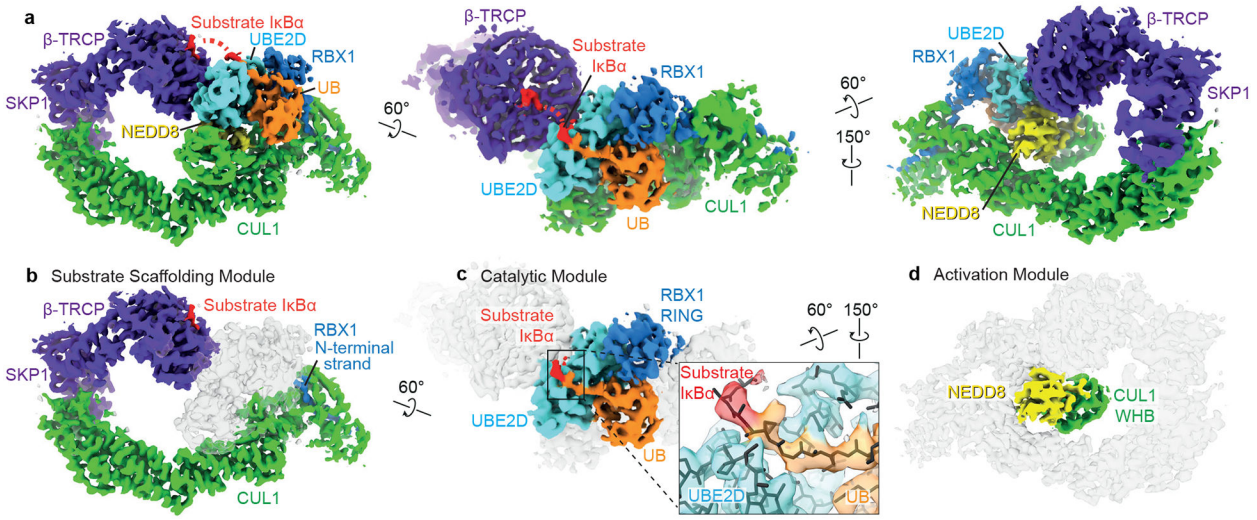

Figure 2 |. Cryo EM structure representing neddylated CRL1$^{β\text{-}TRCP}$-mediated ubiquitin transfer from UBE2D to IκBα substrate

a, Cryo EM density representing neddylated CRL1$^{β\text{-}TRCP}$-UBE2D~ubiquitin-IκBα substrate intermediate, wherein UBE2D~ubiquitin is activated and juxtaposed with substrate. **b**, The substrate scaffolding module connects β-TRCP-bound substrate to the intermolecular cullin-RBX (C/R) domain. **c**, The catalytic module consists of RBX1's RING-UBE2D~UB in the canonical closed activated conformation, and additional density corresponding to the chemical surrogate for substrate undergoing ubiquitylation. **d**, NEDD8 and its covalently-linked CUL1 WHB domain form the activation module.

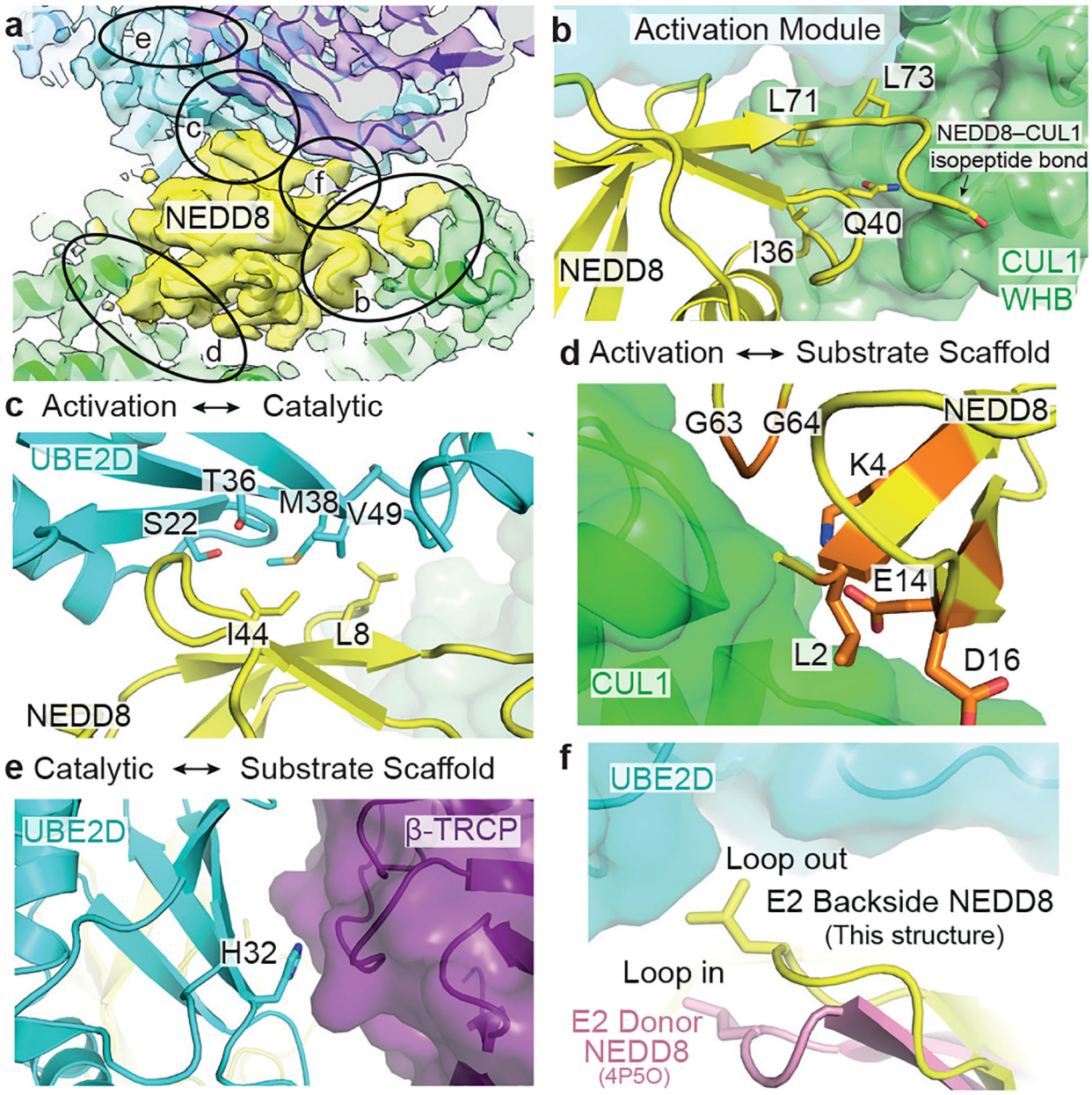

Figure 3 |. Intra- and inter-module interfaces specifying catalytic architecture for ubiquitin priming of substrate by neddylated CRL1$^{\beta\text{-TRCP}}$ with UBE2D

a, Cryo EM density highlighting noncovalent interfaces contributing to the catalytic architecture for neddylated CRL1$^{\beta\text{-TRCP}}$-mediated UB transfer from UBE2D to a substrate. Circled regions correspond to interfaces within activation module, and between activation and catalytic, activation and substrate scaffolding and catalytic and substrate scaffolding modules shown in panels **b-f**. **b**, Close-up of intra-activation module interface, showing NEDD8's buried polar residue Gln40 and Ile36/Leu71/Leu73 hydrophobic patch making noncovalent interactions with CUL1's WHB domain adjacent to the isopeptide bond linking NEDD8 and CUL1. **c**, Close-up of interface between activation and catalytic modules showing key residues at interface between NEDD8 and UBE2D backside. **d**, Close-up

highlighting NEDD8 residues in orange that differ in UB and are at interface with substrate scaffolding module. **e**, Close-up highlighting UBE2D His32 at interface with substrate scaffolding module. **f**, Close-up showing role of NEDD8 Loop-out conformation required for binding UBE2D.

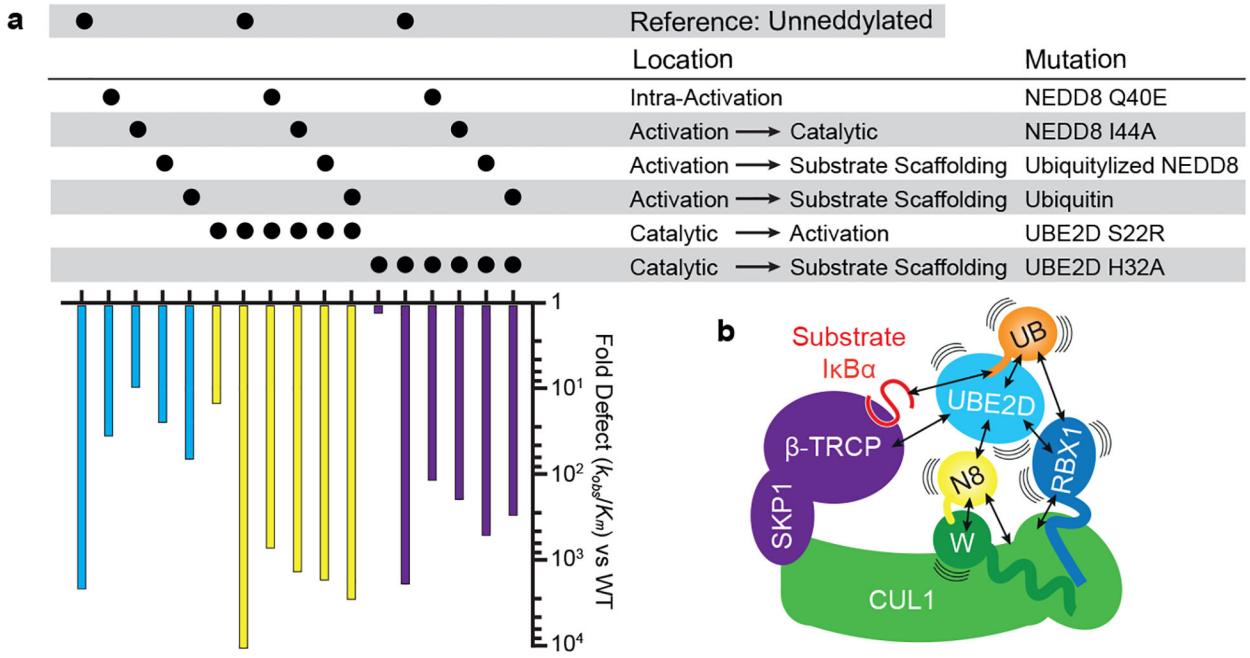

Figure 4 |. Multifarious interactions configuring rapid substrate priming

a, Effects of indicated mutants within activation module, between activation and catalytic, activation and substrate scaffolding and substrate scaffolding and catalytic modules, alone or in combination, on catalytic efficiency of substrate priming as quantified by overall fold difference in k_{obs}/K_m versus wild-type neddylated CRL1$^{\beta\text{-TRCP}}$ and UBE2D-catalyzed ubiquitylation of a peptide substrate. Reactions with unneddylated CRL1$^{\beta\text{-TRCP}}$ serve as a reference, and used CUL1 K720R to prevent obscuring interpretation of results by artifactual UB transfer to CUL1 and resultant artifactual activation of substrate priming. Graphs show average value from two different experiments (technical replicates), for which curve fits and values are provided in Extended data Figure 1 and Extended Data Table 1. **b**, On their own, neddylated CRL1$^{\beta\text{-TRCP}}$ and UBE2D~UB are dynamic, and at an extreme their constituent proteins and/or domains may be substantially waving around. Mobile entities are harnessed in the neddylated CRL1$^{\beta\text{-TRCP}}$-UBE2D~UB-substrate intermediate. There could be multiple routes to the catalytic architecture. It seems equally plausible that the UBE2D~UB intermediate would first encounter RBX1's RING domain or NEDD8, either of which would raise the effective concentration for the other interaction. Likewise, noncovalent-binding between NEDD8 and its linked WHB domain, or with UBE2D's backside, would stabilize NEDD8's Loop-out conformation favoring the other interaction as well. Ultimately, NEDD8, the cullin, and the RBX1-bound UBE2D~UB intermediate make numerous interactions that synergistically establish a distinctive catalytic architecture placing UBE2D adjacent to β-TRCP.